Journal of Sound and Vibration (1998) **210**(4), 529–553

HIGHER-ORDER AVERAGING AND ULTRA-SUBHARMONICS IN FORCED OSCILLATORS

K. YAGASAKI

Department of Mechanical and Systems Engineering, Gifu University, Gifu, Gifu 501-11, *Japan*

(*Received* 24 *January* 1997, *and in final form* 12 *September* 1997)

Generally, various types of ultra-subharmonic motions can be observed in numerical simulations of periodically forced, non-linear oscillators. However, theoretical expositions have been provided only for lower-order subharmonics and superharmonics. For a general class of non-linear oscillators, ultra-subharmonic resonances of order 3/2 and 2/3 are analyzed by applying the higher-order averaging method. The occurrence of ultra-subharmonic motions is theoretically explained, and bifurcation behavior near the ultra-subharmonic resonances is described. The tedious computations required here are implemented by using a package of the computer algebra system, Mathematica, recently developed by the author and his co-worker. Moreover, the fourth-order subharmonic and superharmonic resonance behavior is discussed. An example is presented for the Duffing oscillator with double well potential, and numerical simulation results are given to demonstrate the theoretical results.

1. INTRODUCTION

Consider periodically forced oscillators of the form

$$\ddot{x} + \bar{\delta}\dot{x} + f(x) = \bar{\gamma}\cos\omega t, \tag{1}$$

where $\bar{\delta}$, $\bar{\gamma}$ and ω are positive constants, and f is a sufficiently smooth function of x. When $\bar{\delta} = \bar{\gamma} = 0$, equation (1) is referred to as the *unperturbed system* in the following. The unperturbed phase plane has great variety depending on the form of the function f (see Figure 1 of reference [1]). In particular, if $f(x_0) = 0$ and $\mathrm{d}f(x_0)/\mathrm{d}x > 0$, then there exists a center at $(x, \dot{x}) = (x_0, 0)$ in the phase plane.

If one concentrates on the dynamics near the unperturbed center $(x_0, 0)$, then it is convenient to introduce a local co-ordinate y such that $x = \varepsilon y + x_0$, where $0 < \varepsilon \ll 1$. So equation (1) can be rewritten as a weakly non-linear oscillator

$$\ddot{y} + \bar{\delta}\dot{y} + \omega_0^2 y + \sum_{j=1}^{\infty} \varepsilon^j a_{j+1} y^{j+1} = \gamma\cos\omega t, \tag{2}$$

where $\gamma = \bar{\gamma}/\varepsilon$, $\omega_0^2 = a_1 > 0$ and

$$a_j = \frac{1}{j!}\frac{\mathrm{d}^j f}{\mathrm{d}x^j}(x_0), \qquad j = 1, 2, \ldots. \tag{3}$$

Thus, one only has to study equation (2) in order to discuss the dynamics of equation (1) near the center. Especially, if the ratio of the forcing frequency ω to the natural frequency

0022–460X/98/090529 + 25 $25.00/0/sv971326

ω_0 is close to a rational number, then resonance behavior may occur in equation (2) and hence near the unperturbed center in equation (1).

Many physical and engineering problems can be modelled as systems of the form (1) or (2), and numerous theoretical and numerical studies for them have been done. In particular, the third- or lower-order subharmonic and superharmonic resonances as well as the primary resonance (near the unperturbed centers for equation (1)) were analyzed by using the second-order approximation of perturbation techniques such as the methods of averaging and multiple scales. So it was shown that third- or lower-order subharmonic and superharmonic motions occur as well as resonant harmonic motions. See references [1]–[3] for the details. Moreover, ultra-subharmonics as well as higher-order subharmonics and superharmonics near the associated resonances were observed in numerical simulations (see, e.g., references [4, 5]). However, these numerical observations have not been theoretically explained, unlike lower-order subharmonic and superharmonic resonances.

In this paper a theoretical exposition for the occurrence of ultra-subharmonics in general systems of the form (1) is presented. Moreover, the higher-order subharmonic and superharmonic resonance behavior is discussed. To this end, the higher-order averaging method is applied to equation (2) after some changes of co-ordinates. The details on the higher-order averaging procedure, in which the higher-order terms can be computed by the Lie transform algorithm [6, 7], can be found in reference [8] while its basic idea was described in references [6, 7, 9, 10]. A useful package of the computer algebra system, Mathematica [11], for performing tedious computations required in application of higher-order averaging was also developed in reference [8]. Here the necessary computations are implemented by using the package. It should also be noted that a similar computer algebra program of MACSYMA was available in reference [12] although it uses a different, primitive algorithm.

This paper is arranged as follows. In section 2 an outline of the higher-order averaging method is presented and a general recipe for application of averaging to weakly non-linear systems such as equation (2) near ultra-subharmonic resonances is briefly mentioned. In sections 3 and 4, according to the recipe of section 2, the ultra-subharmonic resonances of order 3/2 and 2/3 near the unperturbed center in equation (1) are discussed by carrying out third-order averaging procedures for equation (2). In section 5, similar third-order averaging analyses are performed for the fourth-order subharmonic and superharmonic resonances. In section 6 an example is presented for the Duffing oscillator with double well potential, and numerical simulation results are given to verify the theoretical results. In conclusion, a summary and some comments are stated in section 7.

2. HIGHER-ORDER AVERAGING

The higher-order averaging method is first reviewed. See reference [8] for the details. Consider systems of the form

$$\dot{\mathbf{x}} = \varepsilon \mathbf{f}(\mathbf{x}, \omega t, \varepsilon), \qquad \mathbf{x} \in \mathbb{R}^n, \qquad 0 < \varepsilon \ll 1, \tag{4}$$

where $\mathbf{f}(\mathbf{x}, \theta, \varepsilon) \in \mathbb{R}^n$ is analytic and of period 2π in θ. $\mathbf{f}(\mathbf{x}, \theta, \varepsilon)$ can be expanded in power series of ε:

$$\mathbf{f}(\mathbf{x}, \theta, \varepsilon) = \sum_{m=1}^{\infty} \frac{\varepsilon^{m-1}}{m!} \mathbf{f}_m(\mathbf{x}, \theta), \tag{5}$$

where $\mathbf{f}_m(\mathbf{x}, \theta)$, $m = 1, 2, \ldots$, are also analytic and of period 2π in θ.

Let $\mathbf{f}^{(m)}(\mathbf{y}, \theta)$, $m = 1, 2, \ldots$, be functions such that they are computed as $\mathbf{f}^{(m)}(\mathbf{y}, \theta) = \mathbf{f}_0^{(m)}(\mathbf{y}, \theta)$ by recursive relations,

$$\mathbf{f}_m^{(0)}(\mathbf{y}, \theta) = \mathbf{f}_m(\mathbf{y}, \theta),$$

$$\mathbf{f}_{m-1}^{(1)}(\mathbf{y}, \theta) = \mathbf{f}_m^{(0)}(\mathbf{y}, \theta) + \sum_{i=0}^{m-2} C_i^{m-1} L_{i+1} \tilde{\mathbf{f}}_{m-i-1}^{(0)}(\mathbf{y}, \theta),$$

$$\mathbf{f}_{m-l}^{(l)}(\mathbf{y}, \theta) = \mathbf{f}_{m-l+1}^{(l-1)}(\mathbf{y}, \theta) + \sum_{i=0}^{m-l} C_i^{m-l} L_{i+1} \tilde{\mathbf{f}}_{m-l-i}^{(l-1)}(\mathbf{y}, \theta) \quad \text{for } l \geqslant 2, \tag{6}$$

where

$$\tilde{\mathbf{f}}_{m-l}^{(l)}(\mathbf{y}, \theta) = \mathbf{f}_{m-l}^{(l)}(\mathbf{y}, \theta) - \omega \frac{\partial \mathbf{w}_m}{\partial \theta}(\mathbf{y}, \theta) \quad \text{for } l \geqslant 1, \tag{7}$$

with

$$C_j^k = \frac{k!}{(k-j)!j!} \quad \text{and} \quad L_i \mathbf{g}(\mathbf{y}, \theta) = \mathrm{D}_y \mathbf{g}(\mathbf{y}, \theta)\mathbf{w}_i(\mathbf{y}, \theta) - \mathrm{D}_y \mathbf{w}_i(\mathbf{y}, \theta)\mathbf{g}(\mathbf{y}, \theta). \tag{8}$$

Using a general theory of the Lie transform [6, 7], one can show that under a transformation of the form

$$\mathbf{x} = \mathbf{y} + \sum_{m=0}^{m_0} \mathbf{w}_m(\mathbf{y}, \omega t), \tag{9}$$

equation (4) is written as

$$\dot{\mathbf{y}} = \sum_{m=1}^{m_0} \frac{\varepsilon^m}{m!} \bar{\mathbf{f}}^{(m)}(\mathbf{y}) + \varepsilon^{m_0+1} \mathbf{g}^{(m)}(\mathbf{y}, \omega t, \varepsilon), \tag{10}$$

where

$$\bar{\mathbf{f}}^{(m)}(\mathbf{y}) = \frac{1}{2\pi} \int_0^{2\pi} \mathbf{f}^{(m)}(\mathbf{y}, \theta)\, \mathrm{d}\theta, \tag{11}$$

and $\mathbf{g}^{(m)}(\mathbf{y}, \theta, \varepsilon)$ is of period 2π in θ. Moreover, the transformation (9) is given by

$$\omega \frac{\partial \mathbf{w}_m}{\partial \theta}(\mathbf{y}, \theta) = \tilde{\mathbf{f}}^{(m)}(\mathbf{y}, \theta), \tag{12}$$

where

$$\tilde{\mathbf{f}}^{(m)}(\mathbf{y}, \theta) = \mathbf{f}^{(m)}(\mathbf{y}, \theta) - \bar{\mathbf{f}}^{m}(\mathbf{y}). \tag{13}$$

When the higher-order term of $O(\varepsilon^{m_0+1})$ is eliminated, equation (10) becomes

$$\dot{\mathbf{y}} = \sum_{m=1}^{m_0} \frac{\varepsilon^m}{m!} \bar{\mathbf{f}}^{(m)}(\mathbf{y}), \tag{14}$$

which is referred to as the m_0-th order averaged system for equation (4).

The first-order averaging theory [9, 10, 13] can easily be extended to the case of higher-order averaging. In particular, a solution $\mathbf{x}(t)$ of the original system (4) can be expressed as

$$\mathbf{x}(t) = \bar{\mathbf{y}}(t) + \sum_{m=1}^{m_0-1} \frac{\varepsilon^m}{m!} \mathbf{w}_m(\bar{\mathbf{y}}(t), \omega t) + O(\varepsilon^{m_0}), \tag{15}$$

by a solution $\bar{\mathbf{y}}(t)$ of the averaged system (14) on the time scale of $O(1/\varepsilon)$ unless the first-order term is zero. If the first-order term is zero, a different estimation is obtained (see references [10, 14]; see also section 3). Hyperbolic fixed points in the averaged system correspond to hyperbolic periodic orbits in the original system, the local stable and unstable manifolds of which can be also approximated by those of the corresponding hyperbolic fixed points in the averaged system. Moreover, hyperbolic periodic orbits in the averaged system correspond to normally hyperbolic invariant 2-tori in the original system and so on.

Consider next periodically forced, weakly non-linear single-degree-of-freedom systems of the form

$$\ddot{x} + \omega_0^2 x = \varepsilon F(x, \dot{x}, \omega t, \varepsilon), \tag{16}$$

where $F(x, \dot{x}, \theta, \varepsilon) \in \mathbb{R}$ is analytical and 2π-periodic in θ. Assume that an ultra-subharmonic resonance occurs such that $\omega/\omega_0 \approx k/l$ with k and l relatively prime integers, and set

$$\varepsilon^j \Omega = (l^2\omega^2 - k^2\omega_0^2)/k^2 \tag{17}$$

with $j \geqslant 1$ an integer. Then, using the van der Pol transformation

$$\begin{pmatrix} u \\ v \end{pmatrix} = \begin{pmatrix} \cos\frac{l}{k}\omega t & -\frac{k}{l\omega}\sin\frac{l}{k}\omega t \\ -\sin\frac{l}{k}\omega t & -\frac{k}{l\omega}\cos\frac{l}{k}\omega t \end{pmatrix} \begin{pmatrix} x \\ \dot{x} \end{pmatrix} \tag{18}$$

in equation (16), one obtains

$$\begin{pmatrix} \dot{u} \\ \dot{v} \end{pmatrix} = -\varepsilon\frac{k}{l\omega}[\varepsilon^{j-1}\Omega x + F(x, \dot{x}, \omega t, \varepsilon)] \begin{pmatrix} \sin\frac{l}{k}\omega t \\ \cos\frac{l}{k}\omega t \end{pmatrix}, \tag{19}$$

where x and $\dot{x}$ are expressed by u and v through equation (18). Equation (19) has the form of equation (4), and hence the averaging method is applicable. See also section 4 of reference [8] for a treatment of multi-degree-of-freedom systems. The package of Mathematica developed in reference [8], "haverage.m", includes two programs which implement the higher-order averaging procedure for equation (4) and the van der Pol transformation for multi-degree-of-freedom systems.

3. ULTRA-SUBHARMONICS OF ORDER 3/2

Consider now the ultra-subharmonic resonance of order 3/2 in equation (2) and equivalently in equation (1). Suppose that $\omega/\omega_0 \approx 3/2$ and set $\varepsilon^2\Omega = (4\omega^2 - 9\omega_0^2)/9$. Replace $\overline{\delta}$ by $\varepsilon^3\delta$ and assume δ and γ to have values of $O(1)$. By letting

$$z = y + \Gamma \cos \omega t, \qquad \Gamma = \gamma/(\omega^2 - \omega_0^2), \tag{20}$$

equation (2) becomes

$$\begin{aligned} \ddot{z} + \omega_0^2 z = & -\varepsilon a_2 (z - \Gamma \cos \omega t)^2 - \varepsilon^2 a_3 (z - \Gamma \cos \omega t)^3 \\ & - \varepsilon^3 [a_4 (z - \Gamma \cos \omega t)^4 + \delta(\dot{z} + \omega\Gamma \sin \omega t)] + O(\varepsilon^4). \end{aligned} \tag{21}$$

The van der Pol transformation (18) with $k = 3$ and $l = 2$ is used to transform equation (21) into a system of the form (4) and the higher-order averaging method is applied. Using the package "haverage.m", one obtains the third-order averaged system

$$\begin{aligned} \dot{u} &= (\varepsilon^2/2\omega)\,[(A_{3/2}\,\Gamma^2 + \tfrac{3}{2}\,\Omega)v + B_{3/2}\,(u^2 + v^2)v] + (\varepsilon^3/2\omega)\,(-\delta\omega u + 2C_{3/2}\,\Gamma^2 uv), \\ \dot{v} &= (\varepsilon^2/2\omega)\,[-(A_{3/2}\,\Gamma^2 + \tfrac{3}{2}\,\Omega)u - B_{3/2}\,(u^2 + v^2)u] + (\varepsilon^3/2\omega)\,[-\delta\omega v + C_{3/2}\,\Gamma^2(u^2 - v^2)], \end{aligned} \tag{22}$$

where

$$\begin{aligned} A_{3/2} &= \tfrac{405}{56}\,(a_2^2/\omega^2) - \tfrac{9}{4}\,a_3, \qquad B_{3/2} = \tfrac{45}{16}\,(a_2^2/\omega^2) - \tfrac{9}{8}\,a_3, \\ C_{3/2} &= \tfrac{15795}{1024}\,(a_2^3/\omega^4) - \tfrac{4455}{512}\,(a_2\,a_3/\omega^2) + \tfrac{9}{8}\,a_4. \end{aligned} \tag{23}$$

Note that the first-order term is zero in the averaged system (22). The transformation (9) is also given by

$$\begin{aligned} \mathbf{w}_1(u, v, \theta) &= \mathbf{w}_{10}(\theta) + \mathbf{w}_{11}(\theta)u + \mathbf{w}_{12}(\theta)v + \mathbf{w}_{13}(\theta)u^2 + \mathbf{w}_{14}(\theta)v^2 + \mathbf{w}_{15}(\theta)uv \\ \mathbf{w}_2(u, v, \theta) &= \mathbf{w}_{20}(\theta) + \mathbf{w}_{21}(\theta)u + \mathbf{w}_{22}(\theta)v + \mathbf{w}_{23}(\theta)u^2 + \mathbf{w}_{24}(\theta)v^2 + \mathbf{w}_{25}(\theta)uv \\ & \quad + \mathbf{w}_{26}(\theta)u^3 + \mathbf{w}_{27}(\theta)v^3 + \mathbf{w}_{28}(\theta)u^2 v + \mathbf{w}_{29}(\theta)uv^2, \end{aligned} \tag{24}$$

where $\theta = \omega t/3$. See the Appendix for the expressions of $\mathbf{w}_{ij}(\theta)$.

The averaged system (22) has a trivial equilibrium at $(u, v) = (0, 0)$, which is always stable. The equilibrium corresponds to a harmonic orbit in equation (2),

$$y = -\Gamma \cos \omega t + \varepsilon\left(-\frac{9a_2\,\Gamma^2}{8\omega^2} + \frac{9a_2\,\Gamma^2}{64\omega^2}\cos 2\omega t\right) + O(\varepsilon^2), \tag{25}$$

and a harmonic orbit in equation (1),

$$x = x_0 - \varepsilon\Gamma \cos \omega t + \varepsilon^2\left(-\frac{9a_2\,\Gamma^2}{8\omega^2} + \frac{9a_2\,\Gamma^2}{64\omega^2}\cos 2\omega t\right) + O(\varepsilon^3). \tag{26}$$

These expressions are easily obtained from equation (24) and also verified by using a regular perturbation technique. Note that the approximate solution in equation (2) can be obtained only to $O(\varepsilon)$ since the first-order averaged term is zero (cf. equation (15)).

In polar co-ordinates, $r = \sqrt{u^2 + v^2}$ and $\phi = \arctan(v/u)$, equation (22) becomes

$$\begin{aligned} \dot{r} &= (\varepsilon^3/2\omega)\,[-\delta\omega r + C_{3/2}\,\Gamma^2 r^2 \sin 3\phi], \\ \dot{\phi} &= (\varepsilon^2/2\omega)\,[-(A_{3/2}\,\Gamma^2 + \tfrac{3}{2}\,\Omega) - B_{3/2}\,r^2] + (\varepsilon^3/2\omega)C_{3/2}\,\Gamma^2 r \cos 3\phi. \end{aligned} \tag{27}$$

The package "haverage.m" can also be used for the derivation of equation (27). Solutions of equation (27) with $r = 0$ correspond to the trivial equilibrium of equation (22).

Suppose that $B_{3/2}$, $C_{3/2} \neq 0$ and that

$$C_{3/2}^2 \Gamma^4[-4B_{3/2}(A_{3/2}\Gamma^2 + \tfrac{3}{2}\Omega) + \varepsilon^2 C_{3/2}^2 \Gamma^4] - 4B_{3/2}^2 \delta^2 \omega^2 > 0,$$

i.e.,

$$-B_{3/2}\Omega > \tfrac{2}{3} A_{3/2} B_{3/2} \Gamma^2 + \tfrac{2}{3}(B_{3/2}^2 \delta^2 \omega^2 / C_{3/2}^2 \Gamma^4) - \tfrac{1}{6}\varepsilon^2 C_{3/2}^2 \Gamma^4. \tag{28}$$

Then equation (27) has fixed points with $r > 0$ at $(r, \phi) = (r_\pm, \phi_\pm + 2j\pi/3)$, $j = 0, 1, 2$, where

$$r_\pm = (1/\sqrt{2}|B_{3/2}|)\{[-2B_{3/2}(A_{3/2}\Gamma^2 + \tfrac{3}{2}\Omega) + \varepsilon^2 C_{3/2}^2 \Gamma^4]$$

$$\pm \varepsilon\sqrt{C_{3/2}^2 \Gamma^4[-4B_{3/2}(A_{3/2}\Gamma^2 + \tfrac{3}{2}\Omega) + \varepsilon^2 C_{3/2}^2 \Gamma^4] - 4B_{3/2}^2 \delta^2 \omega^2}\}^{1/2} \tag{29}$$

and

$$\phi_\pm = \tfrac{1}{3}\arctan(\varepsilon\delta\omega / [(A_{3/2}\Gamma^2 + \tfrac{3}{2}\Omega) + B_{3/2} r_\pm^2]). \tag{30}$$

Note that if condition (28) holds, then the first term in the brace of equation (29), $-2B_{3/2}(A_{3/2}\Gamma^2 + \frac{3}{2}\Omega) + \varepsilon^2 C_{3/2}^2 \Gamma^4$, is positive. The fixed points $(r_+, \phi_+ + 2j\pi/3)$, $j = 0, 1, 2$, are stable and the others are unstable. Each triple of fixed points $(r_\pm, \phi_\pm + 2j\pi/3)$, $j = 0, 1, 2$, corresponds to a *single* ultra-subharmonic orbit of order 3/2 in equation (1),

$$x = x_0 + \varepsilon[-\Gamma \cos \omega t + r_\pm \cos(\tfrac{2}{3}\omega t + \phi_\pm)] + O(\varepsilon^2), \tag{31}$$

with the same stability type.

The two triples of fixed points appear or disappear at three saddle-node bifurcations [13, 15] when

$$\Omega = -\tfrac{2}{3} A_{3/2}\Gamma^2 - \tfrac{2}{3}(B_{3/2}\delta^2\omega^2 / C_{3/2}^2 \Gamma^4) + \tfrac{1}{6}\varepsilon^2 (C_{3/2}^2 \Gamma^4 / B_{3/2}). \tag{32}$$

By noting that $\omega = \frac{3}{2}\omega_0 + O(\varepsilon^2)$, and $\omega_0^2 = a_1$, the saddle-node bifurcation set (32) can be expressed as

$$\Omega = -\tfrac{2}{3}\bar{A}_{3/2}\Gamma^2 - \tfrac{3}{2}(a_1 \bar{B}_{3/2}\delta^2 / \bar{C}_{3/2}^2 \Gamma^4) + O(\varepsilon^2), \tag{33}$$

where

$$\bar{A}_{3/2} = \tfrac{45}{14}(a_2^2/a_1) - \tfrac{9}{4}a_3, \qquad \bar{B}_{3/2} = \tfrac{5}{4}(a_2^2/a_1) - \tfrac{9}{8}a_3,$$

$$\bar{C}_{3/2} = \tfrac{195}{64}(a_2^3/a_1^2) - \tfrac{495}{128}(a_2 a_3/a_1) + \tfrac{9}{8}a_4. \tag{34}$$

Equation (33) also represents an approximate saddle-node bifurcation set in equation (1) at which stable and unstable ultra-subharmonic orbits of order 3/2 given by equation (31) appear or disappear.

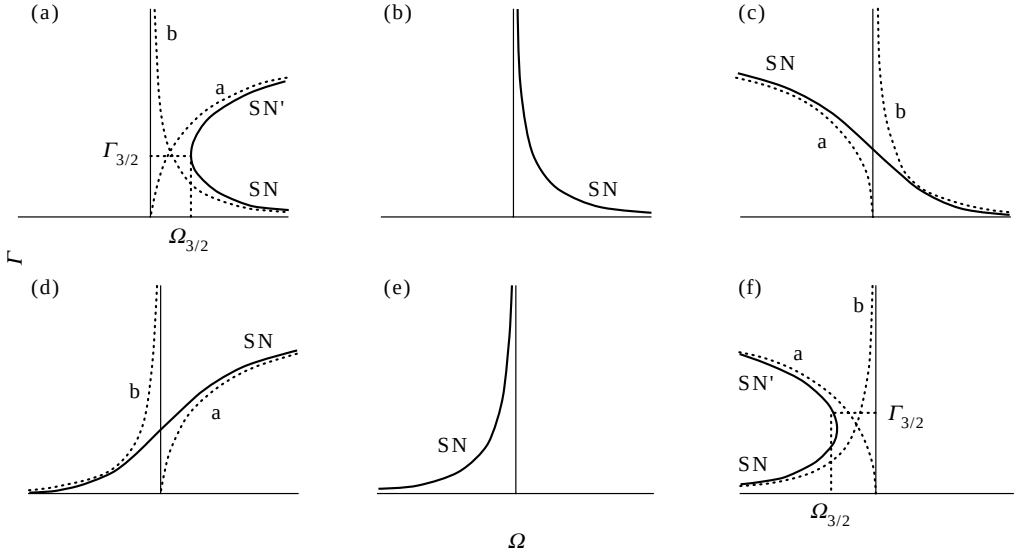

Figure 1. Saddle-node bifurcation sets near the ultra-subharmonic resonance of order 3/2 in equation (1) when the control parameters are Γ and Ω. (a) $\overline{A}_{3/2} < 0$ and $\overline{B}_{3/2} < 0$; (b) $\overline{A}_{3/2} = 0$ and $\overline{B}_{3/2} < 0$; (c) $\overline{A}_{3/2} > 0$ and $\overline{B}_{3/2} < 0$; (d) $\overline{A}_{3/2} < 0$ and $\overline{B}_{3/2} > 0$; (e) $\overline{A}_{3/2} = 0$ and $\overline{B}_{3/2} > 0$; (f) $\overline{A}_{3/2} > 0$ and $\overline{B}_{3/2} > 0$. SN and SN′, respectively, denote super- and subcritical saddle-node bifurcations when Γ (i.e., the forcing amplitude $\bar{\gamma}$) is changed. The broken curves labeled a and b, respectively, represent the graphs of $\Omega = -\frac{2}{3}\overline{A}_{3/2}\Gamma^2$ and $\Omega = -\frac{3}{2}(a_1\overline{B}_{3/2}\delta^2/\overline{C}_{3/2}\Gamma^4)$.

The approximate saddle-node bifurcation curves in the (Ω, Γ)-space are shown in Figure 1, and the associated bifurcation diagrams for the averaged system (27) are shown in Figure 2. Here $\Gamma_{3/2}^6 = \frac{9}{2}(a_1\,\overline{B}_{3/2}\,\delta^2/\overline{A}_{3/2}\,\overline{C}_{3/2}^2)$ and $\Omega_{3/2}^3 = -\frac{9}{2}(a_1\,\overline{A}_{3/2}^2\,\overline{B}_{3/2}\,\delta^2/\overline{C}_{3/2}^2)$. Note that the bifurcation curves are similar to those of third-order subharmonics (cf. Figure 6 of reference [1]). When Γ is increased while the other parameters are fixed (or equivalently only the forcing amplitude $\bar{\gamma}$ is changed), both supercritical and subcritical saddle-node bifurcations can occur if $\overline{A}_{3/2}\,\overline{B}_{3/2} > 0$, and only supercritical saddle-node bifurcations can occur if $\overline{A}_{3/2}\,\overline{B}_{3/2} \leqslant 0$. The phase portraits of the averaged system (22) are also sketched in Figure 3 for some parameter values. Here the numerical computations were performed by using a software called "Dynamics" [16].

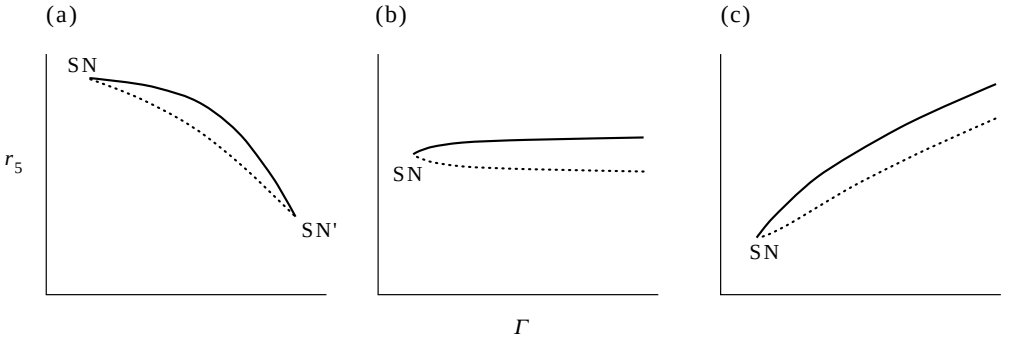

Figure 2. Bifurcation diagrams for the averaged system (27) when the control parameter is Γ. (a) $\overline{A}_{3/2} < 0$, $\overline{B}_{3/2} < 0$, $\Omega > \Omega_{3/2}$, or $\overline{A}_{3/2} > 0$, $\overline{B}_{3/2} > 0$, $\Omega < \Omega_{3/2}$; (b) $\overline{A}_{3/2} = 0$, $\overline{B}_{3/2}\Omega < 0$; (c) $\overline{A}_{3/2}\overline{B}_{3/2} < 0$. Note that no bifurcations occur in other cases. The points with $r > 0$ correspond to ultra-subharmonics of order 3/2 in equation (1). SN and SN′ denote super- and subcritical saddle-node bifurcations. Stable and unstable orbits are also shown as solid and broken lines, respectively.

4. ULTRA-SUBHARMONICS OF ORDER 2/3

Next consider the ultra-subharmonic resonance of order 2/3. Suppose that $\omega/\omega_0 \approx 2/3$, and set $\varepsilon^2\Omega = (9\omega^2 - 4\omega_0^2)/4$. Application of the van der Pol transformation (18) with $k = 2$ and $l = 3$ and the third-order averaging method to equation (21) yields

$$\dot{u} = (\varepsilon^2/2\omega)\,[(A_{2/3}\,\Gamma^2 + \tfrac{2}{3}\,\Omega)v + B_{2/3}\,(u^2 + v^2)v] + (\varepsilon^3/2\omega)\,(-\delta\omega u - C_{2/3}\,\Gamma^3 v),$$

$$\dot{v} = (\varepsilon^2/2\omega)\,[-(A_{2/3}\,\Gamma^2 + \tfrac{2}{3}\,\Omega)u - B_{2/3}\,(u^2 + v^2)u] + (\varepsilon^3/2\omega)\,(-C_{2/3}\,\Gamma^3 u - \delta\omega v), \quad (35)$$

which is expressed in polar co-ordinates as

$$\dot{r} = (\varepsilon^3/2\omega)\,[-\delta\omega r - C_{2/3}\,\Gamma^3 r \sin 2\phi],$$

$$\dot{\phi} = (\varepsilon^2/2\omega)\,[-(A_{2/3}\,\Gamma^2 + \tfrac{2}{3}\,\Omega) - B_{2/3}\,r^2] - (\varepsilon^2/2\omega)C_{2/3}\,\Gamma^3 \cos 2\phi, \quad (36)$$

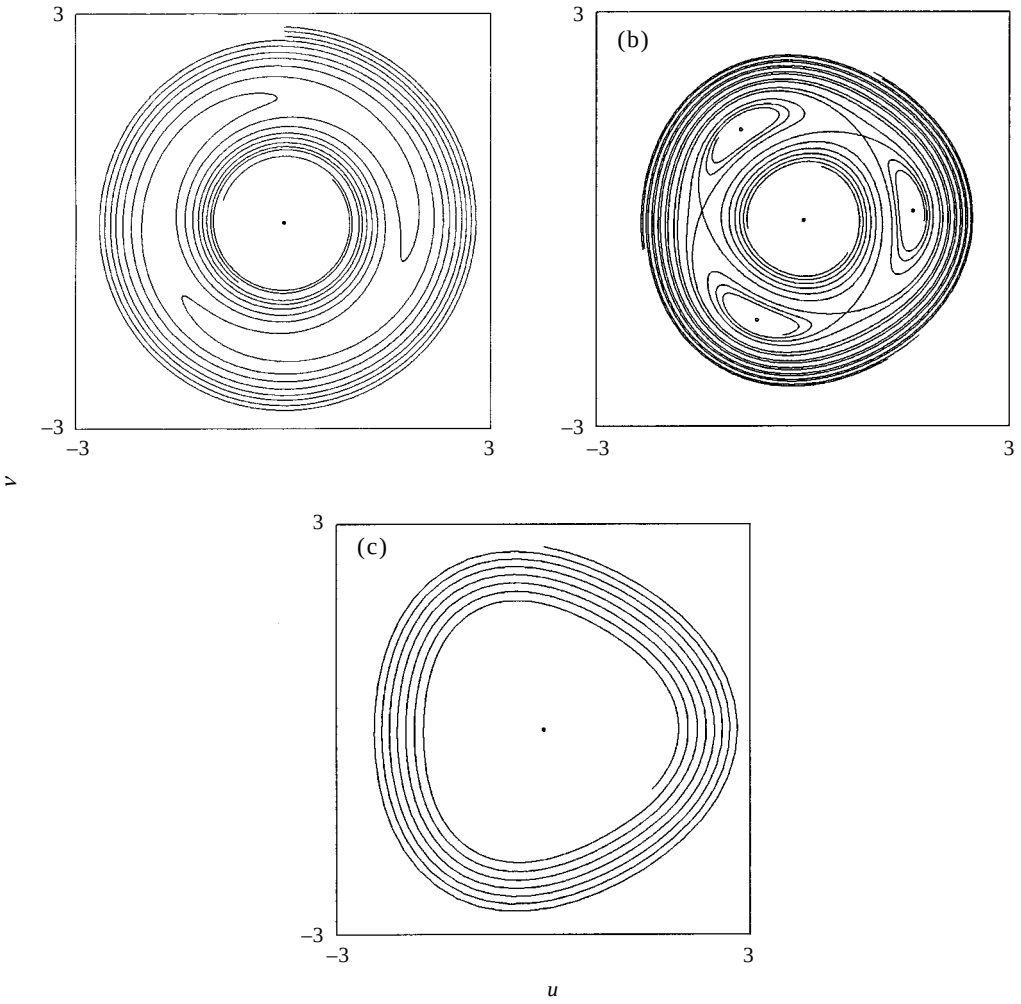

Figure 3. Phase portraits of the averaged system (22) for $A_{3/2} = 171/14 \approx 12{\cdot}21428571$, $B_{3/2} = 9/2(= 4{\cdot}5)$, $C_{3/2} = 945/64(= 14{\cdot}765625)$, $\Omega = -10$ and $\delta\omega = 3\sqrt{2}/2 \approx 2{\cdot}12132034$. (a) $\Gamma = 0{\cdot}2$; (b) $\Gamma = 0{\cdot}6$; (c) $\Gamma = 1{\cdot}2$. The dots (●) represent stable fixed points. The parameter values are included in the cases of Figures 1(f) and 2(a). When Γ is changed, three supercritical saddle-node bifurcations simultaneously occur at $\Gamma \approx 0{\cdot}28536493$ and three subcritical saddle-node bifurcations simultaneously occur at $\Gamma \approx 1{\cdot}1127972$. Similar phase portraits are also obtained in other cases.

where

$$A_{2/3} = \tfrac{25}{54}(a_2^2/\omega^2) - a_3, \qquad B_{2/3} = \tfrac{20}{81}(a_2^2/\omega^2) - \tfrac{1}{2}a_3,$$
$$C_{2/3} = \tfrac{5}{1134}(a_2^3/\omega^4) - \tfrac{215}{1134}(a_2 a_3/\omega^2) + \tfrac{1}{3}a_4. \tag{37}$$

Here the package "haverage.m" was also used. The averaged system (35) has a trivial equilibrium at $(u, v) = (0, 0)$, which corresponds to a harmonic orbit in equation (1),

$$x = x_0 - \varepsilon\Gamma\cos\omega t + \varepsilon^2\left(-\frac{2a_2\Gamma^2}{9\omega^2} + \frac{2a_2\Gamma^2}{7\omega^2}\cos 2\omega t\right) + O(\varepsilon^3). \tag{38}$$

The equilibrium is stable if

$$(A_{2/3}\Gamma^2 + \tfrac{2}{3}\Omega)^2 > \varepsilon^2[C_{2/3}^2\Gamma^6 - \delta^2\omega^2], \tag{39}$$

and unstable if

$$(A_{2/3}\Gamma^2 + \tfrac{2}{3}\Omega)^2 < \varepsilon^2[C_{2/3}^2\Gamma^6 - \delta^2\omega^2]. \tag{40}$$

Suppose that $B_{2/3}$, $C_{2/3} \neq 0$ and that

$$C_{2/3}^2\Gamma^6 - \delta^2\omega^2 > 0 \quad \text{and} \quad B_{2/3}[-(A_{2/3}\Gamma^2 + \tfrac{2}{3}\Omega) \pm \varepsilon\sqrt{C_{2/3}^2\Gamma^6 - \delta^2\omega^2}] > 0. \tag{41}$$

Then equation (36) has non-trivial fixed points at $(r, \phi) = (r_\pm, \phi_\pm)$ and $(r_\pm, \phi_\pm + \pi)$, where

$$r_\pm = \sqrt{(1/B_{2/3})[-(A_{2/3}\Gamma^2 + \tfrac{2}{3}\Omega) \pm \varepsilon\sqrt{C_{2/3}^2\Gamma^6 - \delta^2\omega^2}]} \tag{42}$$

and

$$\phi_\pm = \tfrac{1}{2}\arctan(\varepsilon\delta\omega/[(A_{2/3}\Gamma^2 + \tfrac{2}{3}\Omega) + B_{2/3}r_\pm^2]). \tag{43}$$

Moreover, when $B_{2/3} > 0$ (resp. $B_{2/3} < 0$), the fixed points (r_+, ϕ_+), $(r_+, \phi_+ + \pi)$ are stable (resp. unstable) and the others are unstable (resp. stable). Each pair of fixed points $(r_\pm, \phi_\pm)$, $(r_\pm, \phi_\pm + \pi)$ corresponds to a single ultra-subharmonic orbit of order 2/3 in equation (1),

$$x = x_0 + \varepsilon[-\Gamma\cos\omega t + r_\pm\cos(\tfrac{3}{2}\omega t + \phi_\pm)] + O(\varepsilon^2), \tag{44}$$

with the same stability type.

The two pairs of fixed points appear or disappear at two saddle-node bifurcations when

$$C_{2/3}^2\Gamma^6 - \delta^2\omega^2 = 0, \tag{45}$$

if $-B_{2/3}(A_{2/3}\Gamma^2 + \tfrac{2}{3}\Omega) > 0$. On the other hand, if the first condition in equation (41) holds and

$$-(A_{2/3}\Gamma^2 + \tfrac{2}{3}\Omega) \pm \varepsilon\sqrt{C_{2/3}^2\Gamma^6 - \delta^2\omega^2} = 0, \tag{46}$$

then a pitchfork bifurcation [13, 15] occurs at $r = 0$ (i.e., $(u, v) = (0, 0)$) and the pair of fixed points, $(r_\pm, \phi_\pm)$, $(r_\pm, \phi_\pm + \pi)$, disappears or appears there. Since $\omega = \tfrac{2}{3}\omega_0 + O(\varepsilon^2)$ and $\omega_0^2 = a_1$, the saddle-node bifurcation set (45) and pitchfork bifurcation sets (46) can be expressed as

$$\Gamma^6 = \tfrac{4}{9}(a_1\delta^2/\overline{C}_{2/3}^2) + O(\varepsilon^2) \tag{47}$$

and

$$\Omega = \tfrac{3}{2}[-\overline{A}_{2/3}\Gamma^2 \pm \varepsilon\sqrt{\overline{C}_{2/3}^2\Gamma^6 - \tfrac{4}{9}a_1\delta^2}] + O(\varepsilon^2), \tag{48}$$

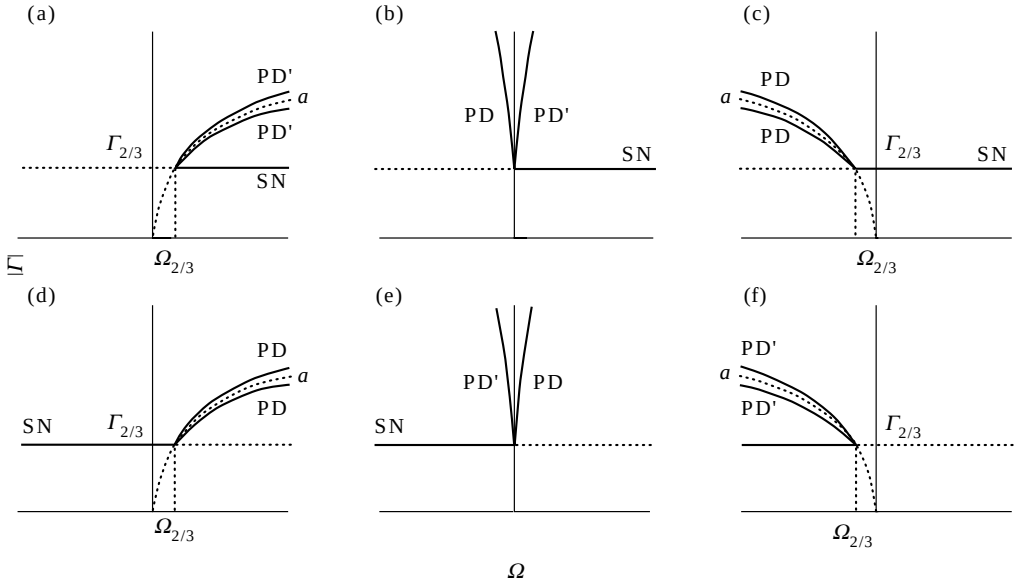

Figure 4. Saddle-node and period doubling bifurcation sets near the ultra-subharmonic resonance of order 2/3 in equation (1) when the control parameters are $|\Gamma|$ and Ω. (a) $\bar{A}_{2/3} < 0$ and $\bar{B}_{2/3} < 0$; (b) $\bar{A}_{2/3} = 0$ and $\bar{B}_{2/3} < 0$; (c) $\bar{A}_{2/3} > 0$ and $\bar{B}_{2/3} < 0$; (d) $\bar{A}_{2/3} < 0$ and $\bar{B}_{2/3} > 0$; (e) $\bar{A}_{2/3} = 0$ and $\bar{B}_{2/3} > 0$; (f) $\bar{A}_{2/3} > 0$ and $\bar{B}_{2/3} > 0$. PD and PD′, respectively, denote super- and subcritical period doubling bifurcations, and SN denotes supercritical saddle-node bifurcations when $|\Gamma|$ (i.e., the forcing amplitude $\bar{\gamma}$) is changed. The broken curves labeled *a* represent the graph of $\Omega = -\frac{3}{2}\bar{A}_{2/3}\Gamma^2$.

respectively, where

$$\bar{A}_{2/3} = \tfrac{25}{24}(a_2^2/a_1) - a_3, \qquad \bar{B}_{2/3} = \tfrac{5}{9}(a_2^2/a_1) - \tfrac{1}{2}a_3,$$

$$\bar{C}_{2/3} = \tfrac{5}{224}(a_2^3/a_1^2) - \tfrac{215}{504}(a_2 a_3/a_1) + \tfrac{1}{3}a_4. \tag{49}$$

Note that the pitchfork bifurcations correspond to period doubling bifurcations [13, 15] of the harmonic orbit given by equation (38) to the ultra-subharmonic orbits of order 2/3 given by equation (44) in equation (1): the stability of the harmonic orbit changes (cf. equations (39), (40) and (46)) and the ultra-subharmonic orbits appear or disappear there. See also references [1, 3]. So equations (47) and (48), respectively, represent approximate saddle-node and period doubling bifurcation sets for ultra-subharmonics of order 2/3 in equation (1).

The approximate saddle-node and period doubling bifurcation curves in the $(\Omega, |\Gamma|)$-space are shown in Figure 4, and the associated bifurcation diagrams for the averaged system (36) are shown in Figure 5. Here $\Gamma_{2/3}^6 = \frac{4}{9}(a_1\,\delta^2/\bar{C}_{2/3}^2)$ and $\Omega_{2/3}^3 = -\frac{3}{2}(a_1\,\bar{A}_{2/3}^3\,\delta^2/\bar{C}_{2/3}^2)$. Note that at $\omega t = 0 \mod 2\pi$ the ultra-subharmonic orbits of order 2/3 take $x = x_0 + \varepsilon(-\Gamma + r_\pm \cos\phi_\pm) + O(\varepsilon^2)$ or $x = x_0 + \varepsilon(-\Gamma - r_\pm \cos\phi_\pm) + O(\varepsilon^2)$ while the harmonic orbit takes only $x = x_0 - \varepsilon\Gamma + O(\varepsilon^2)$. Thus, when the forcing amplitude $\bar{\gamma}$ is increased while the other parameters are fixed, the stable and unstable ultra-subharmonic orbits appear or disappear in several manners, depending on the parameter values: they are created at supercritical saddle-node or period doubling bifurcations, and annihilated at subcritical period doubling bifurcations. The phase portraits of the averaged system (35) are sketched in Figure 6 for some parameter values. Again, the software "Dynamics" was used to draw these pictures.

Analyses similar to those of the preceding and this sections may also reveal other *purely* ultra-subharmonic resonance motions such that $\omega/\omega_0 \approx k/l$ with $k, l > l$ relatively prime integers. However, application of third- or fourth-order averaging to these cases only yields uninteresting or insufficient averaged systems: they have only trivial equilibria or they are degenerate. So fifth- or higher-order averaging is required for such analyses. Some results on these ultra-subharmonic resonances will also be reported elsewhere.

5. HIGHER-ORDER SUBHARMONICS AND SUPERHARMONICS

It is plausible to consider that the higher-order averaging method can shed light on not only purely ultra-subharmonic resonance motions, but also higher-order subharmonic and superharmonic resonance motions. In this section, to demonstrate its usefulness in the latter cases, fourth-order subharmonic and superharmonic resonances are discussed by using the third-order averaging procedure. Fifth- or higher-order subharmonic and superharmonic resonances can also be similarly analyzed although fourth- or higher-order averaging is required.

5.1. FOURTH-ORDER SUBHARMONICS

Consider the fourth-order subharmonic resonance, $\omega/\omega_0 \approx 4$, and set $\varepsilon^2\Omega = (\omega^2 - 16\omega_0^2)/16$. Application of the van der Pol transformation (18) with $k = 4$ and

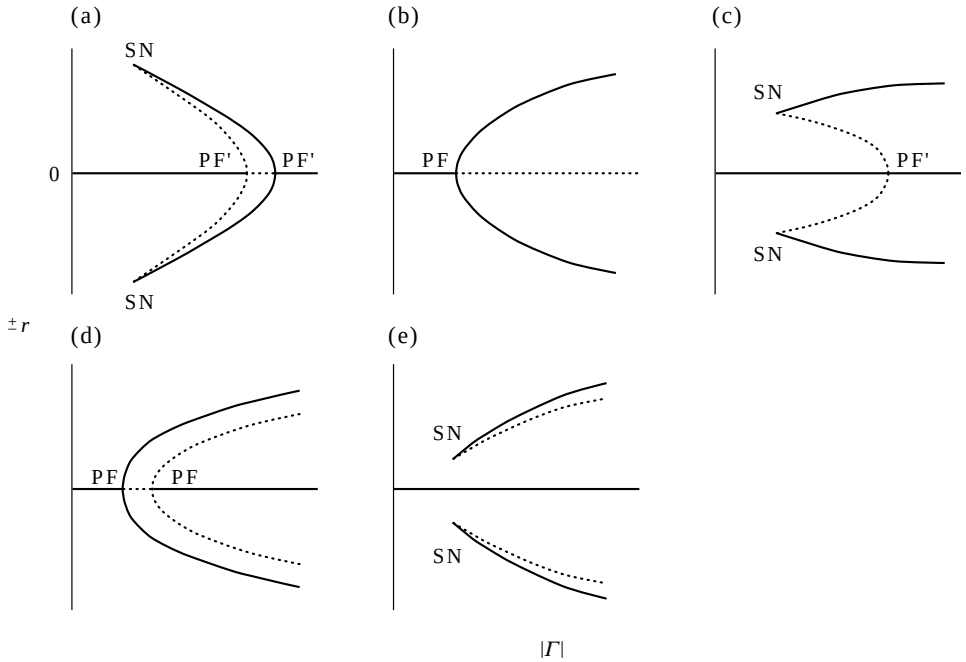

Figure 5. Bifurcation diagrams for the averaged system (36) when the control parameter is $|\Gamma|$. (a) $\bar{A}_{2/3} < 0$, $\bar{B}_{2/3} < 0$, $\Omega > \Omega_{2/3}$ or $\bar{A}_{2/3} > 0$, $\bar{B}_{2/3} > 0$, $\Omega < \Omega_{2/3}$; (b) $\bar{A}_{2/3} = 0$, $\bar{B}_{2/3} < 0$, $\Omega < 0$ or $\bar{A}_{2/3} = 0$, $\bar{B}_{2/3} > 0$, $\Omega > 0$; (c) $\bar{A}_{2/3} = 0$, $\bar{B}_{2/3} < 0$, $\Omega > 0$ or $\bar{A}_{2/3} = 0$, $\bar{B}_{2/3} > 0$, $\Omega < 0$; (d) $\bar{A}_{2/3} > 0$, $\bar{B}_{2/3} < 0$, $\Omega < \Omega_{2/3}$ or $\bar{A}_{2/3} < 0$, $\bar{B}_{2/3} > 0$, $\Omega > \Omega_{2/3}$; (e) $\bar{A}_{2/3} > 0$, $\bar{B}_{2/3} < 0$, $\Omega > \Omega_{2/3}$ or $\bar{A}_{2/3} < 0$, $\bar{B}_{2/3} > 0$, $\Omega < \Omega_{2/3}$. The points with $r > 0$ correspond to ultra-subharmonics of order 2/3 in equation (1), while the points with $r = 0$ correspond to harmonics. PF and PF′, respectively, denote super- and subcritical pitchfork bifurcations. See also the caption of Figure 2.

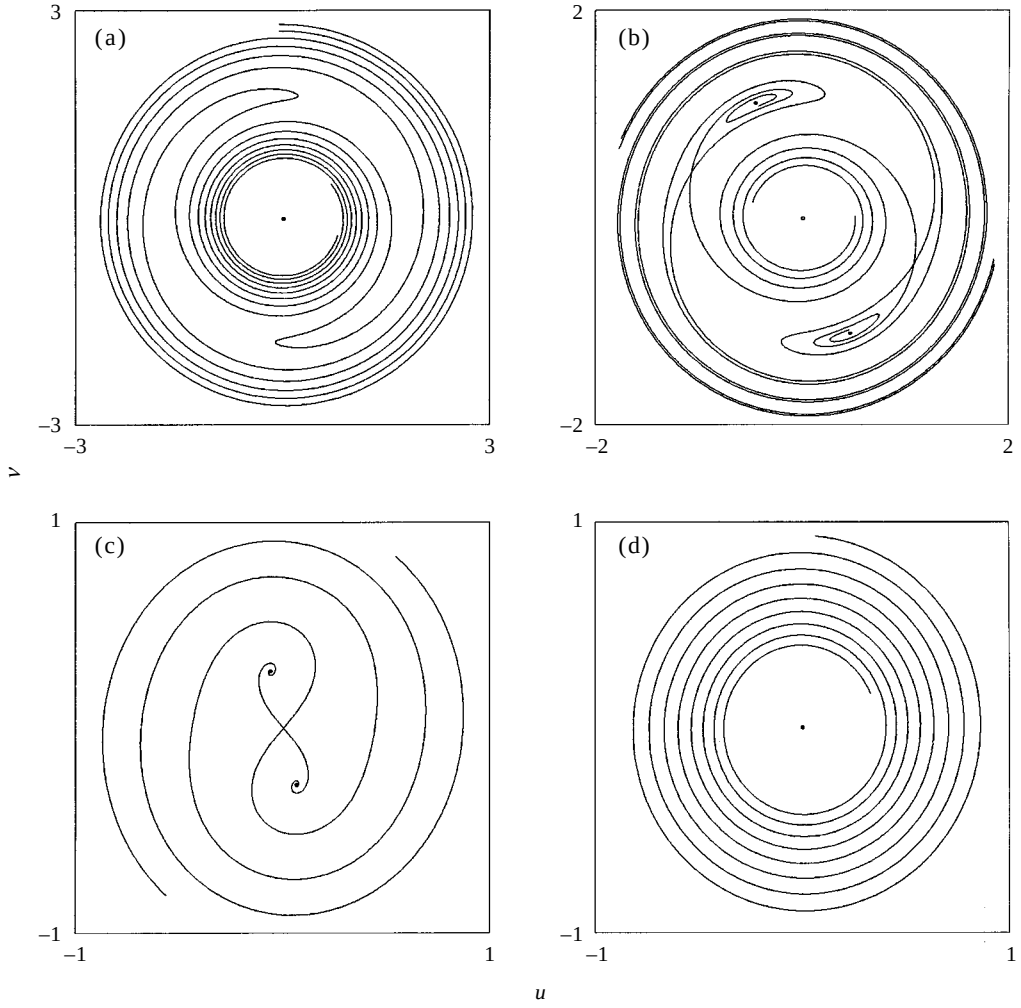

Figure 6. Phase portraits of the averaged system (35) for $A_{2/3} = 59/16(= 3{\cdot}6875)$, $B_{2/3} = 2$, $C_{2/3} = -1315/1688 \approx -0{\cdot}48921131$, $\Omega = -15$ and $\delta\omega = 2\sqrt{2}/3 \approx 0{\cdot}94280904$. (a) $\Gamma = -1$; (b) $\Gamma = -1{\cdot}4$; (c) $\Gamma = -1{\cdot}65$; (d) $\Gamma = -2$. These parameter values are included in the cases of Figures 4(f) and 5(a). When $|\Gamma|$ is changed, two supercritical saddle-node bifurcations simultaneously occur at $|\Gamma| \approx 1{\cdot}2447607$, and subcritical pitchfork bifurcations occur at $|\Gamma| \approx 1{\cdot}6310537$ and at $|\Gamma| \approx 1{\cdot}66351311$. See also the caption of Figure 3.

$l = 1$ and the third-order averaging method to equation (21) yields

$$\dot{u} = (\varepsilon^2/2\omega)\,[(A_{4/1}\,\Gamma^2 + 4\Omega)v + B_{4/1}\,(u^2 + v^2)v] + (\varepsilon^3/2\omega)\,[-\delta\omega u - C_{4/1}\,\Gamma(3u^2 - v^2)v],$$

$$\dot{v} = (\varepsilon^2/2\omega)\,[-(A_{4/1}\,\Gamma^2 + 4\Omega)u - B_{4/1}\,(u^2 + v^2)u] + (\varepsilon^3/2\omega)\,[-\delta\omega v - C_{4/1}\,\Gamma(u^2 - 3v^2)u], \tag{50}$$

which is expressed in polar co-ordinates as

$$\dot{r} = (\varepsilon^3/2\omega)\,[-\delta\omega r - C_{4/1}\,\Gamma r^3 \sin 4\phi],$$

$$\dot{\phi} = (\varepsilon^2/2\omega)\,[-(A_{4/1}\,\Gamma^2 + 4\Omega) - B_{4/1}\,r^2] - (\varepsilon^3/2\omega)C_{4/1}\,\Gamma r^2 \cos 4\phi, \tag{51}$$

where

$$A_{4/1} = \tfrac{160}{3}(a_2^2/\omega^2) - 6a_3, \qquad B_{4/1} = \tfrac{160}{3}(a_2^2/\omega^2) - 3a_3,$$
$$C_{4/1} = \tfrac{1280}{9}(a_2^3/\omega^4) + 40(a_2\, a_3/\omega^2) + 2a_4. \tag{52}$$

The averaged system (50) has a trivial equilibrium at $(u, v) = (0, 0)$, which is always stable and corresponds to a harmonic orbit in equation (1),

$$x = x_0 - \varepsilon\Gamma\cos\omega t + \varepsilon^2\left(-\frac{8a_2\,\Gamma^2}{\omega^2} + \frac{8a_2\,\Gamma^2}{63\omega^2}\cos 2\omega t\right) + O(\varepsilon^3). \tag{53}$$

If $B_{4/1},\ C_{4/1} \neq 0$,

$$-B_{4/1}\,(A_{4/1}\,\Gamma^2 + 4\Omega) > 0 \tag{54}$$

and

$$C_{4/1}^2\,\Gamma^2(A_{4/1}\,\Gamma^2 + 4\Omega)^2 > B_{4/1}^2\,\delta^2\omega^2 - \varepsilon^2 C_{4/1}^2\,\Gamma^2\delta^2\omega^2, \tag{55}$$

then equation (51) has non-trivial fixed points at $(r, \phi) = (r_\pm, \phi_\pm + j\pi/2)$, $j = 0, 1, 2, 3$, where

$$r_\pm = \left\{\frac{1}{B_{4/1}^2 - \varepsilon^2 C_{4/1}^2\,\Gamma^2}\,[-B_{4/1}\,(A_{4/1}\,\Gamma^2 + 4\Omega)\right.$$
$$\left. \pm\,\varepsilon\sqrt{(C_{4/1}\,\Gamma)^2(A_{4/1}\,\Gamma^2 + 4\Omega)^2 - B_{4/1}^2\,\delta^2\omega^2 + \varepsilon^2 C_{4/1}^2\,\Gamma^2\delta^2\omega^2}]\right\}^{1/2} \tag{56}$$

and

$$\phi_\pm = \tfrac{1}{4}\arctan\,(-\delta\omega/[(A_{4/1}\,\Gamma^2 + 4\Omega) + B_{4/1}\,r_\pm^2]). \tag{57}$$

The fixed points $(r_+, \phi_+ + j\pi/2)$, $j = 0, 1, 2, 3$, are stable and the others are unstable. Each set of fixed points corresponds to a single fourth-order subharmonic orbit in equation (1),

$$x = x_0 + \varepsilon[-\Gamma\cos\omega t + r_\pm\cos(\tfrac{1}{4}\omega t + \phi_\pm)] + O(\varepsilon^2), \tag{58}$$

with the same stability type. The two sets of fixed points appear or disappear at four saddle-node bifurcations when condition (54) holds and

$$C_{4/1}^2\,\Gamma^2(A_{4/1}\,\Gamma^2 + 4\Omega)^2 = B_{4/1}^2\,\delta^2\omega^2 - \varepsilon^2 C_{4/1}^2\,\Gamma^2\delta^2\omega^2. \tag{59}$$

Note that if condition (55) holds, then equality does not hold instead of inequality in equation (55) since $B_{4/1} \neq 0$. By using the relation $\omega = 4\sqrt{a_1} + O(\varepsilon^2)$, the saddle-node bifurcation set (59) can be expressed as

$$\Omega = -\tfrac{1}{4}\,\bar{A}_{4/1}\,\Gamma^2 - \sqrt{a_1}\,\bar{B}_{4/1}\,\delta/|\bar{C}_{4/1}|\Gamma + O(\varepsilon^2), \tag{60}$$

which represents an approximate saddle-node bifurcation set of fourth-order subharmonic orbits, where

$$\bar{A}_{4/1} = \tfrac{10}{3}(a_2^2/a_1) - 6a_3, \qquad \bar{B}_{4/1} = \tfrac{10}{3}(a_2^2/a_1) - 3a_3,$$
$$\bar{C}_{4/1} = \tfrac{5}{9}(a_2^3/a_1^2) + \tfrac{5}{2}(a_2\, a_3/a_1) + 2a_4. \tag{61}$$

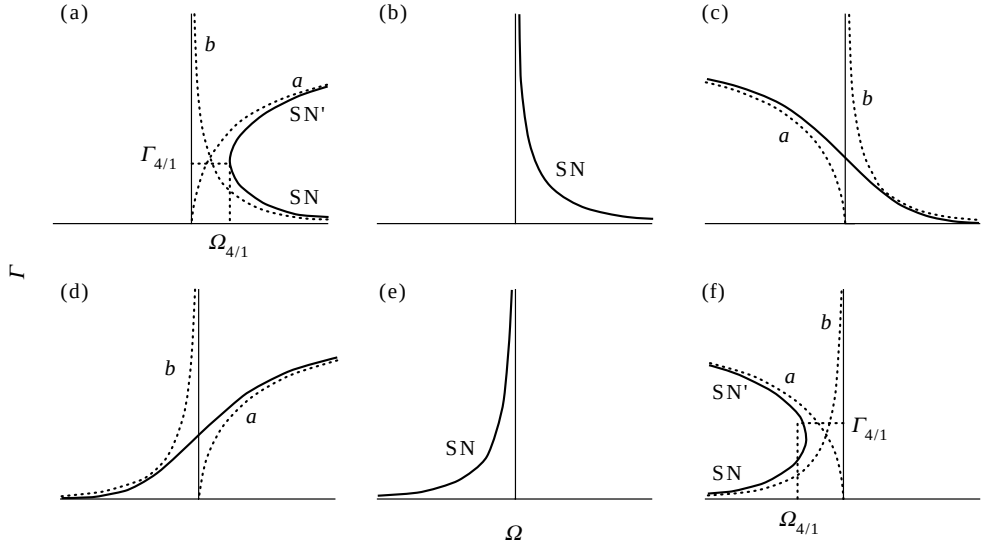

Figure 7. Saddle-node bifurcation sets near the fourth-order subharmonic resonance in equation (1) when the control parameters are Γ and Ω. (a) $\bar{A}_{4/1} < 0$ and $\bar{B}_{4/1} < 0$; (b) $\bar{A}_{4/1} = 0$ and $\bar{B}_{4/1} < 0$; (c) $\bar{A}_{4/1} > 0$ and $\bar{B}_{4/1} < 0$; (d) $\bar{A}_{4/1} < 0$ and $\bar{B}_{4/1} > 0$; (e) $\bar{A}_{4/1} = 0$ and $\bar{B}_{4/1} > 0$; (f) $\bar{A}_{4/1} > 0$ and $\bar{B}_{4/1} \geq 0$. The broken curves labeled a and b, respectively, represent the graphs of $\Omega = -\frac{1}{4}\bar{A}_{4/1}\Gamma^2$ and $\Omega = -(\sqrt{a_1}\bar{B}_{4/1}\delta/|\bar{C}_{4/1}|\Gamma)$. See also the caption of Figure 1.

Figures 7 and 8, respectively, show the approximation saddle-node bifurcation sets (60) in the (Ω, Γ)-space and associated bifurcation diagrams for the averaged system (51). Here $\Gamma_{4/1}^3 = 2(\sqrt{a_1}\,\bar{B}_{4/1}\,\delta/\bar{A}_{4/1}\,|\bar{C}_{4/1}\,|)$ and $\Omega_{4/1}^3 = -\frac{27}{16}(a_1\,\bar{A}_{4/1}\,\bar{B}_{4/1}^2\,\delta^2/\bar{C}_{4/1}^2)$. Thus, the bifurcation curve is similar to those of third-order subharmonics and ultra-subharmonics of order 3/2 (cf. Figure 6 of reference [1] and Figure 1): when $\bar{\gamma}$ is increased, fourth-order subharmonics appear or disappear at supercritical or subcritical saddle-node bifurcations. The phase portraits of the averaged system (50) drawn by the software "Dynamics" are also shown in Figure 9.

5.2. FOURTH-ORDER SUPERHARMONICS

Next consider the fourth-order superharmonic resonance, $\omega/\omega_0 \approx 1/4$, and set $\varepsilon^2\Omega = 16\omega^2 - \omega_0^2$. Application of the van der Pol transformation (18) with $k = 1$ and $l = 4$

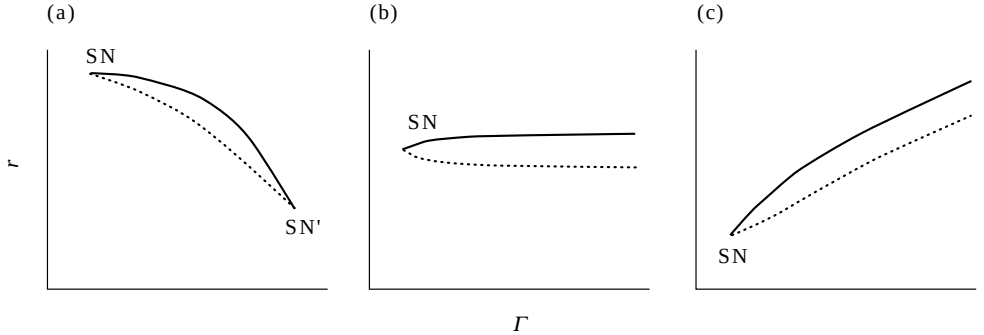

Figure 8. Bifurcation diagrams for the averaged system (51) when the control parameter is Γ. (a) $\bar{A}_{4/1} < 0$, $\bar{B}_{4/1} < 0$, $\Omega > \Omega_{4/1}$, or $\bar{A}_{4/1} > 0$, $\bar{B}_{4/1} > 0$, $\Omega < \Omega_{4/1}$; (b) $\bar{A}_{4/1} = 0$, $\bar{B}_{4/1}\Omega < 0$; (c) $\bar{A}_{4/1}\bar{B}_{4/1} < 0$. The points with $r > 0$ correspond to fourth-order subharmonics in equation (1). See also the caption of Figure 2.

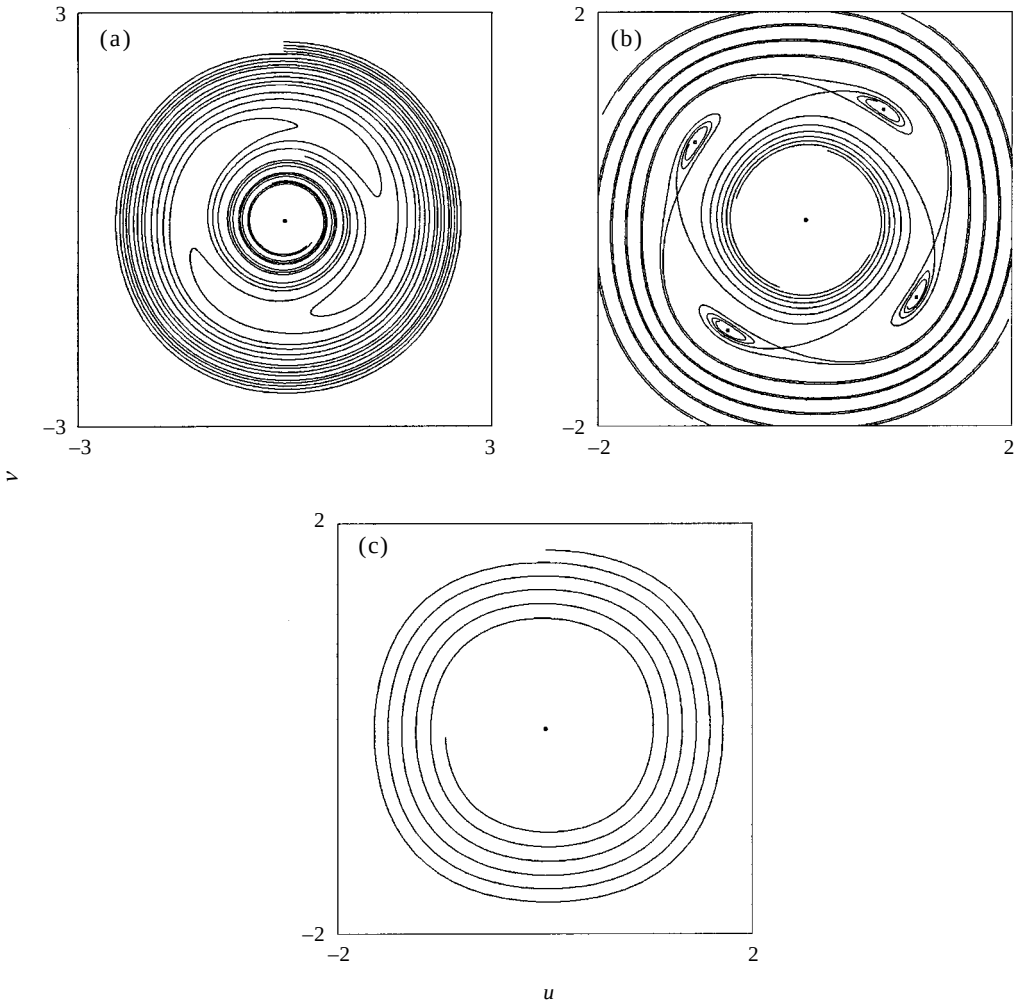

Figure 9. Phase portraits of the averaged system (50) for $A_{4/1} = 9$, $B_{4/1} = 12$, $C_{4/1} = 15/2(= 7{\cdot}5)$, $\Omega = -6$ and $\delta\omega = 4\sqrt{2} \approx 5{\cdot}65685425$. (a) $\Gamma = 0{\cdot}3$; (b) $\Gamma = 0{\cdot}7$; (c) $\Gamma = 2$. These parameter values are included in the cases of Figures 7(f) and 8(a). When Γ is increased, four supercritical saddle-node bifurcations simultaneously occur at $\Gamma \approx 0{\cdot}40122646$ and four subcritical saddle-node bifurcations simultaneously occur at $\Gamma \approx 1{\cdot}7953490$. See also the caption of Figure 3.

and the third-order averaging method to equation (21) yields

$$\dot{u} = (\varepsilon^2/2\omega)\,[(A_{1/4}\,\Gamma^2 + \tfrac{1}{4}\,\Omega)v + B_{1/4}\,(u^2 + v^2)v] - (\varepsilon^3/2\omega)\delta\omega u,$$

$$\dot{v} = (\varepsilon^2/2\omega)\,[-(A_{1/4}\,\Gamma^2 + \tfrac{1}{4}\,\Omega)u - B_{1/4}\,(u^2 + v^2)u] + (\varepsilon^2/2\omega)\,(-\delta\omega v + C_{1/4}\,\Gamma^4), \quad (62)$$

which is expressed in polar co-ordinates as

$$\dot{r} = (\varepsilon^2/2\omega)\,[-\delta\omega r + C_{1/4}\,\Gamma^4 \sin\phi],$$

$$\dot{\phi} = (\varepsilon^2/2\omega)\,[-(A_{1/4}\,\Gamma^2 + \tfrac{1}{4}\,\Omega) - B_{1/4}\,r^2] + (\varepsilon^3/2\omega)C_{1/4}\,\Gamma^4 \cos\phi/r, \quad (63)$$

where

$$A_{1/4} = \tfrac{95}{4032}\,(a_2^2/\omega^2) - \tfrac{3}{8}\,a_3, \qquad B_{1/4} = \tfrac{5}{384}\,(a_2^2/\omega^2) - \tfrac{3}{16}\,a_3,$$
$$C_{1/4} = \tfrac{55}{32256}\,(a_2^3/\omega^4) - \tfrac{15}{896}\,(a_2\,a_3/\omega^2) + \tfrac{1}{32}\,a_4. \tag{64}$$

Equations (62) and (63) have the same forms as the averaged systems for equation (1) near the primary resonance. See section 2.1 of reference [1]. Therefore, an analysis similar to that given there reveals the dynamical and bifurcation behavior in equations (62) and (63).

Suppose that $B_{1/4} \neq 0$. Let r_0 be a solution of the algebraic equation

$$(\varepsilon\delta\omega r)^2 + [(A_{1/4}\,\Gamma^2 + \tfrac{1}{4}\,\Omega)r + B_{1/4}\,r^3]^2 = (\varepsilon C_{1/4}\,\Gamma^4)^2 \tag{65}$$

and let

$$\phi_0 = \arctan\,(\varepsilon\delta\omega/[(A_{1/4}\,\Gamma^2 + \tfrac{1}{4}\,\Omega) + B_{1/4}\,r_0^2]), \tag{66}$$

then (r_0, ϕ_0) is a fixed point of equation (63) and corresponds to a fourth-order superharmonic orbit in equation (1),

$$x = x_0 + \varepsilon[-\Gamma\,\cos\,\omega t + r_0\cos\,(4\omega t + \phi_0)] + O(\varepsilon^2). \tag{67}$$

The fixed points appear or disappear at a saddle-node bifurcation when

$$\varepsilon^2 C_{1/4}^2\,\Gamma^8 = \{-2(A_{1/4}\,\Gamma^2 + \tfrac{1}{4}\,\Omega)\,[(A_{1/4}\,\Gamma^2 + \tfrac{1}{4}\,\Omega)^2 + 9\varepsilon^2\delta^2\omega^2]$$
$$\pm\, 2[(A_{1/4}\,\Gamma^2 + \tfrac{1}{4}\,\Omega)^2 - 3\varepsilon^2\delta^2\omega^2]^{3/2}\}/27B_{1/4}. \tag{68}$$

The saddle-node bifurcation sets (68) can be expressed as

$$\varepsilon^2 C_{1/4}^2\,\Gamma^8 = -\varepsilon^2\delta^2\omega^2(A_{1/4}\,\Gamma^2 + \tfrac{1}{4}\,\Omega)/B_{1/4} + O(\varepsilon^4) \tag{69}$$

and

$$\varepsilon^2 C_{1/4}^2\,\Gamma^8 = [-4(A_{1/4}\,\Gamma^2 + \tfrac{1}{4}\,\Omega)^3 - 9\varepsilon^2\delta^2\omega^2(A_{1/4}\,\Gamma^2 + \tfrac{1}{4}\,\Omega)]/27B_{1/4} + O(\varepsilon^4), \tag{70}$$

i.e.,

$$\Omega = -4\bar{A}_{1/4}\,\Gamma^2 - 64\bar{B}_{1/4}\,\bar{C}_{1/4}^2\,\Gamma^8/a_1\,\delta^2 + O(\varepsilon^2) \tag{71}$$

and

$$\Omega = -4\bar{A}_{1/4}\,\Gamma^2 + O(\varepsilon^2), \tag{72}$$

where

$$\bar{A}_{1/4} = \tfrac{95}{252}\,(a_2^2/a_1) - \tfrac{3}{8}\,a_3, \qquad \bar{B}_{1/4} = \tfrac{5}{24}\,(a_2^2/a_1) - \tfrac{3}{16}\,a_3,$$
$$\bar{C}_{1/4} = \tfrac{55}{126}\,(a_2^3/a_1^2) - \tfrac{15}{56}\,(a_2\,a_3/a_1) + \tfrac{1}{32}\,a_4. \tag{73}$$

Here the relation $\omega = \frac{1}{4}\sqrt{a_1}$ was used. Note that $(A_{1/4}\,\Gamma^2 + \frac{1}{4}\,\Omega)^2 \geqslant 3\varepsilon^2\delta^2\omega^2$ by equation (68), so that

$$\Gamma^8 \geqslant \pm\,\frac{\sqrt{3}}{72}\,\varepsilon a_1^{3/2}\,\delta^3/\bar{B}_{1/4}\,\bar{C}_{1/4}^2, \tag{74}$$

where the upper choice of the sign is taken for $\bar{B}_{1/4} > 0$ and the lower choice for $\bar{B}_{1/4} < 0$. Equations (71) and (72) also represent approximate saddle-node bifurcation sets of fourth-order superharmonic orbits.

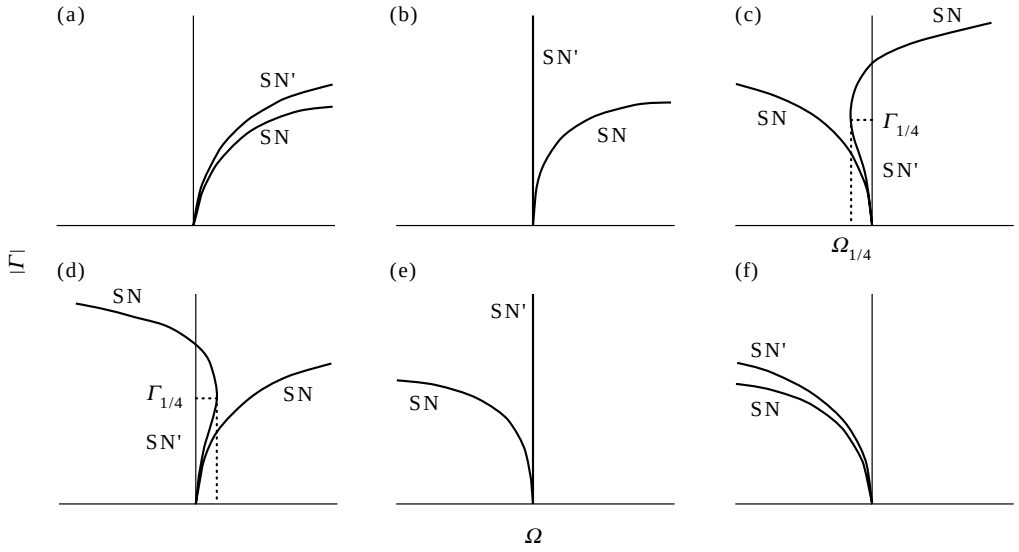

Figure 10. Saddle-node bifurcation sets near the fourth-order superharmonic resonance in equation (1) when the control parameters are $|\Gamma|$ and Ω. (a) $\bar{A}_{1/4} < 0$ and $\bar{B}_{1/4} < 0$; (b) $\bar{A}_{1/4} = 0$ and $\bar{B}_{1/4} < 0$; (c) $\bar{A}_{1/4} > 0$ and $\bar{B}_{1/4} < 0$; (d) $\bar{A}_{1/4} < 0$ and $\bar{B}_{1/4} > 0$; (e) $\bar{A}_{1/4} = 0$ and $\bar{B}_{1/4} > 0$; (f) $\bar{A}_{1/4} > 0$ and $\bar{B}_{1/4} > 0$. See also the caption of Figure 1.

Figures 10 and 11, respectively, show the approximation saddle-node bifurcation sets in the $(\Omega, |\Gamma|)$-space and associated bifurcation diagrams for the averaged system (63). Here $\Gamma_{1/4}^6 = -\frac{1}{64}(a_1 \bar{A}_{1/4}\, \delta^2/\bar{B}_{1/4}\, \bar{C}_{1/4}^2)$ and $\Omega_{1/4}^3 = \frac{27}{4096}(a_1^2\, \bar{A}_{1/4}^5\, \delta^4/\bar{B}_{1/4}^2\, \bar{C}_{1/4}^4)$. Thus, when $\bar{\gamma}$ is increased, fourth-order superharmonics are created at a supercritical saddle-node bifurcation and annihilated at a subcritical saddle-node bifurcation like third- or lower-order superharmonics near the associated resonances, but the bifurcation set structure is a little different from those near third- or lower-order superharmonic resonances (cf. reference [1]). The phase portraits of the averaged system (62) drawn by the software "Dynamics" are also shown in Figure 12.

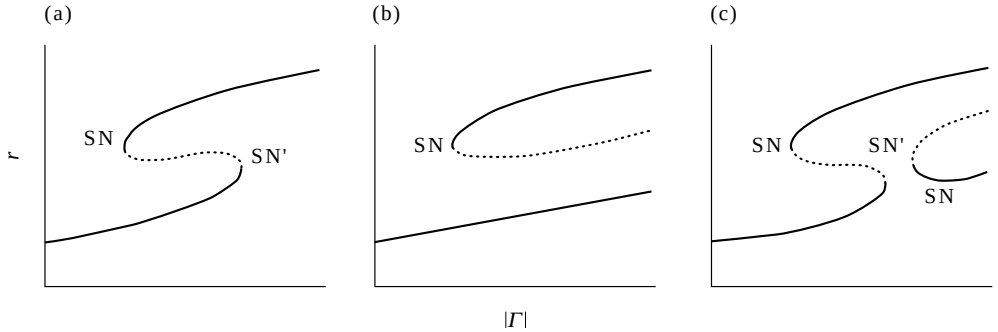

Figure 11. Bifurcation diagrams for the averaged system (63) when the control parameter is $|\Gamma|$. (a) $\bar{A}_{1/4} < 0$, $\bar{B}_{1/4} < 0$, $\Omega > 0$, or $\bar{A}_{1/4} > 0$, $\bar{B}_{1/4} > 0$, $\Omega < 0$; (b) one of the following four conditions holds: (i) $\bar{A}_{1/4} \geqslant 0$, $\bar{B}_{1/4} < 0$, $\Omega > 0$; (ii) $\bar{A}_{1/4} \leqslant 0$, $\bar{B}_{1/4} > 0$, $\Omega < 0$; (iii) $\bar{A}_{1/4} > 0$, $\bar{B}_{1/4} < 0$, $\Omega < \Omega_{1/4}$; (iv) $\bar{A}_{1/4} \leqslant 0$, $\bar{B}_{1/4} > 0$, $\Omega > \Omega_{1/4}$; (c) $\bar{A}_{1/4} > 0$, $\bar{B}_{1/4} < 0$, $\Omega_{1/4} < \Omega < 0$ or $\bar{A}_{1/4} < 0$, $\bar{B}_{1/4} > 0$, $0 < \Omega < \Omega_{1/4}$. The points with $r > 0$ correspond to fourth-order superharmonics in equation (1). See also the caption of Figure 2.

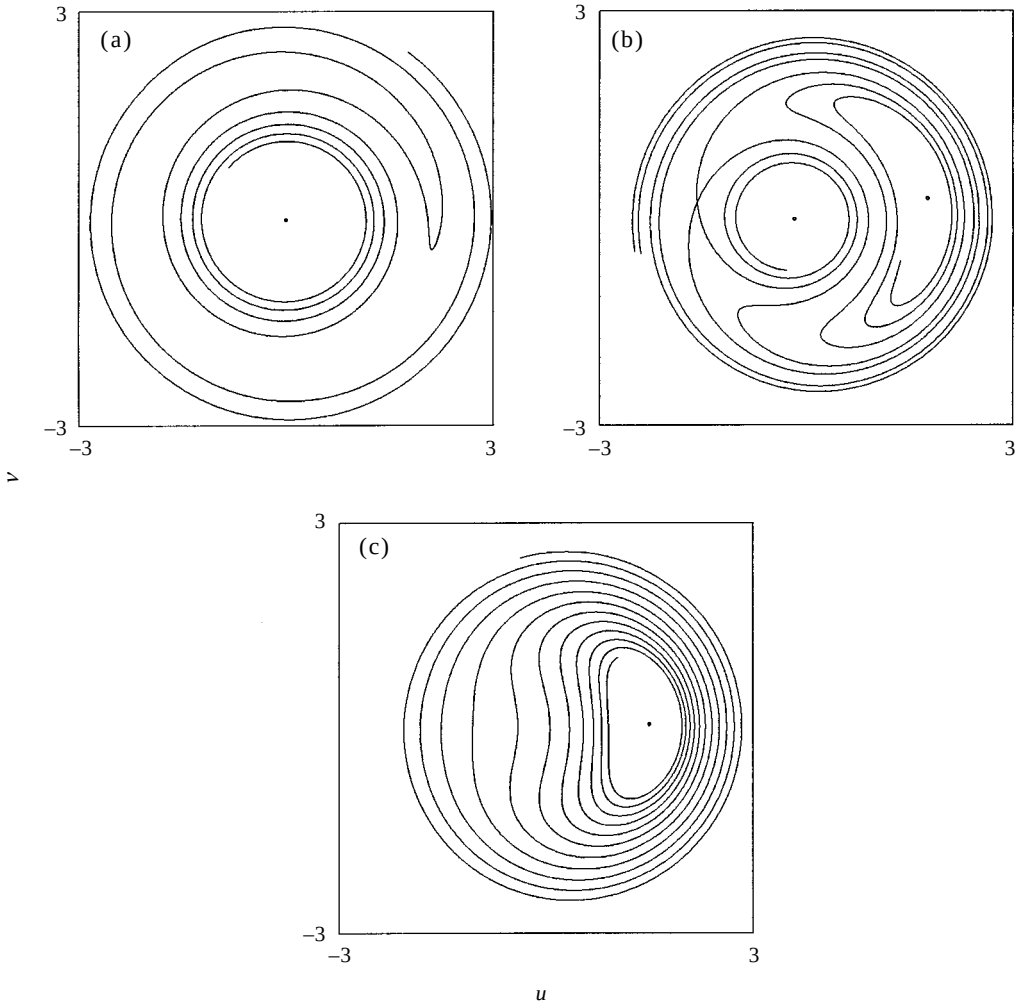

Figure 12. Phase portraits of the averaged system (62) for $A_{1/4} = 37/28 \approx 1{\cdot}32142857$, $B_{1/4} = 3/4(= 0{\cdot}75)$, $C_{1/4} = 285/112(= 2{\cdot}54464286)$, $\Omega = -15$ and $\delta\omega = \sqrt{2}/4 \approx 0{\cdot}35355339$. (a) $\Gamma = -0{\cdot}5$; (b) $\Gamma = -1{\cdot}1$; (c) $\Gamma = -1{\cdot}5$. These parameter values are included in the cases of Figures 10(f) and 11(a). When Γ is increased, a supercritical saddle-node bifurcation occurs at $\Gamma \approx 0{\cdot}72756049$ and a subcritical saddle-node bifurcation occurs at $\Gamma \approx 1{\cdot}3203928$. See also the caption of Figure 3.

6. AN EXAMPLE

To illustrate the above theoretical results, the Duffing oscillator with double well potential,

$$\ddot{x} + \bar{\delta}\dot{x} - x + x^3 = \bar{\gamma}\cos\omega t, \tag{75}$$

i.e., the case of $f(x) = -x + x^3$, is studied as an example. The unperturbed system has two centers at $(x, \dot{x}) = (\pm 1, 0)$. The third- or lower-order subharmonic and superharmonic resonance motions near the centers in equation (75) as well as the primary resonance motions were discussed in a similar fashion by using the second-order averaging method in reference [1].

For the two centers one has $a_1 = 2$, $a_2 = \pm 3$, $a_3 = 1$ and $a_j = 0$, $j \geqslant 4$. So the values of

TABLE 1

The values of $\overline{A}_{k/l}$, $\overline{B}_{k/l}$ *and* $\overline{C}_{k/l}$ *for the centers* $(x, \dot{x}) = (\pm 1, 0)$ *in equation* (75)

(k, l)	$\overline{A}_{k/l}$	$\overline{B}_{k/l}$	$\overline{C}_{k/l}$
(3, 2)	$\frac{171}{14}$	$\frac{9}{2}$	$\pm\frac{945}{64}$
(2, 3)	$\frac{59}{16}$	2	$\mp\frac{1315}{2688}$
(4, 1)	9	12	$\pm\frac{15}{2}$
(1, 4)	$\frac{37}{28}$	$\frac{3}{4}$	$\pm\frac{285}{112}$

the parameters $\overline{A}_{k/l}$, $\overline{B}_{k/l}$ and $\overline{C}_{k/l}$, defined by equations (34), (49), (61) and (73), are computed from these values. See Table 1 for the parameter values.

Figure 13 shows the approximate saddle-node and period-doubling bifurcation sets near the unperturbed centers, obtained by the above third-order averaging analyses of sections 3–5, in the $(\omega, \bar{\gamma})$-space. The bifurcation sets near the ultra-subharmonic resonances of

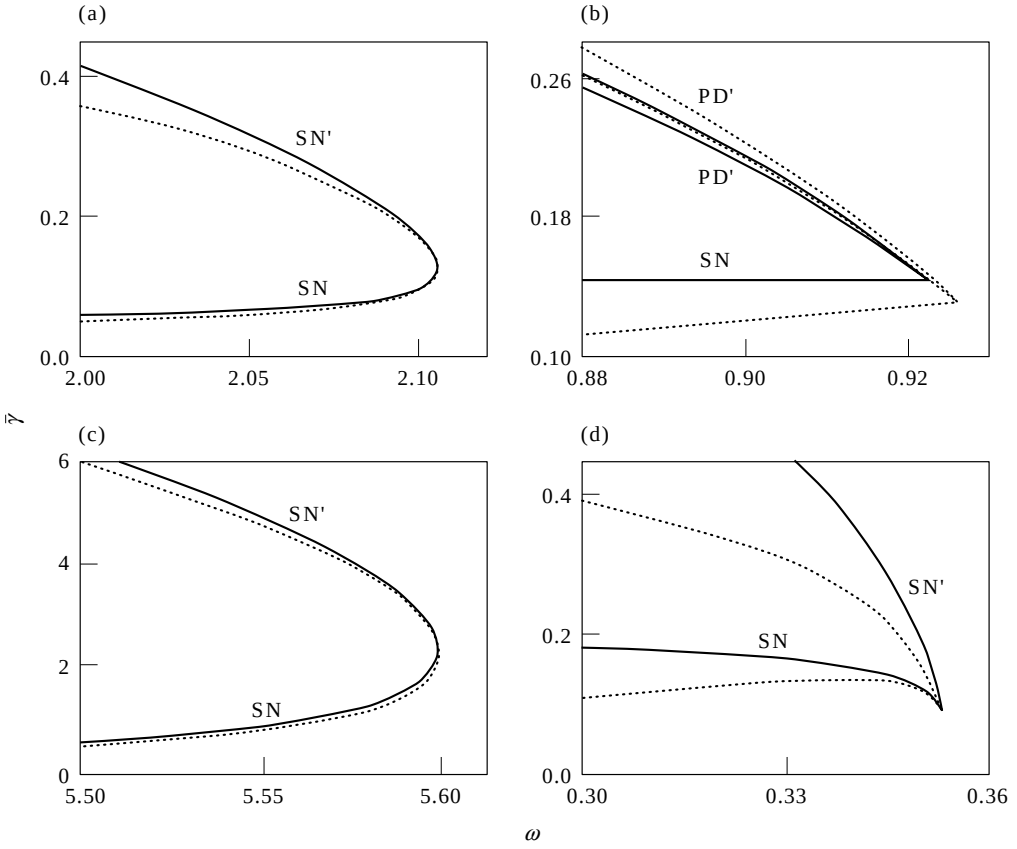

Figure 13. Bifurcation sets near the unperturbed centers in equation (75) when the control parameters are $\bar{\gamma}$ and ω. (a) Saddle-node bifurcations near the ultra-subharmonic resonance of order 3/2; (b) saddle-node and period-doubling bifurcations near the ultra-subharmonic resonance of order 2/3; (c) saddle-node bifurcations near the fourth-order subharmonic resonance; (d) saddle-node bifurcations near the fourth-order superharmonic resonance. Bifurcation sets predicted by the third-order averaging theory are shown as solid lines, and numerically computed bifurcation sets are shown as broken lines. See also the captions of Figures 1 and 4.

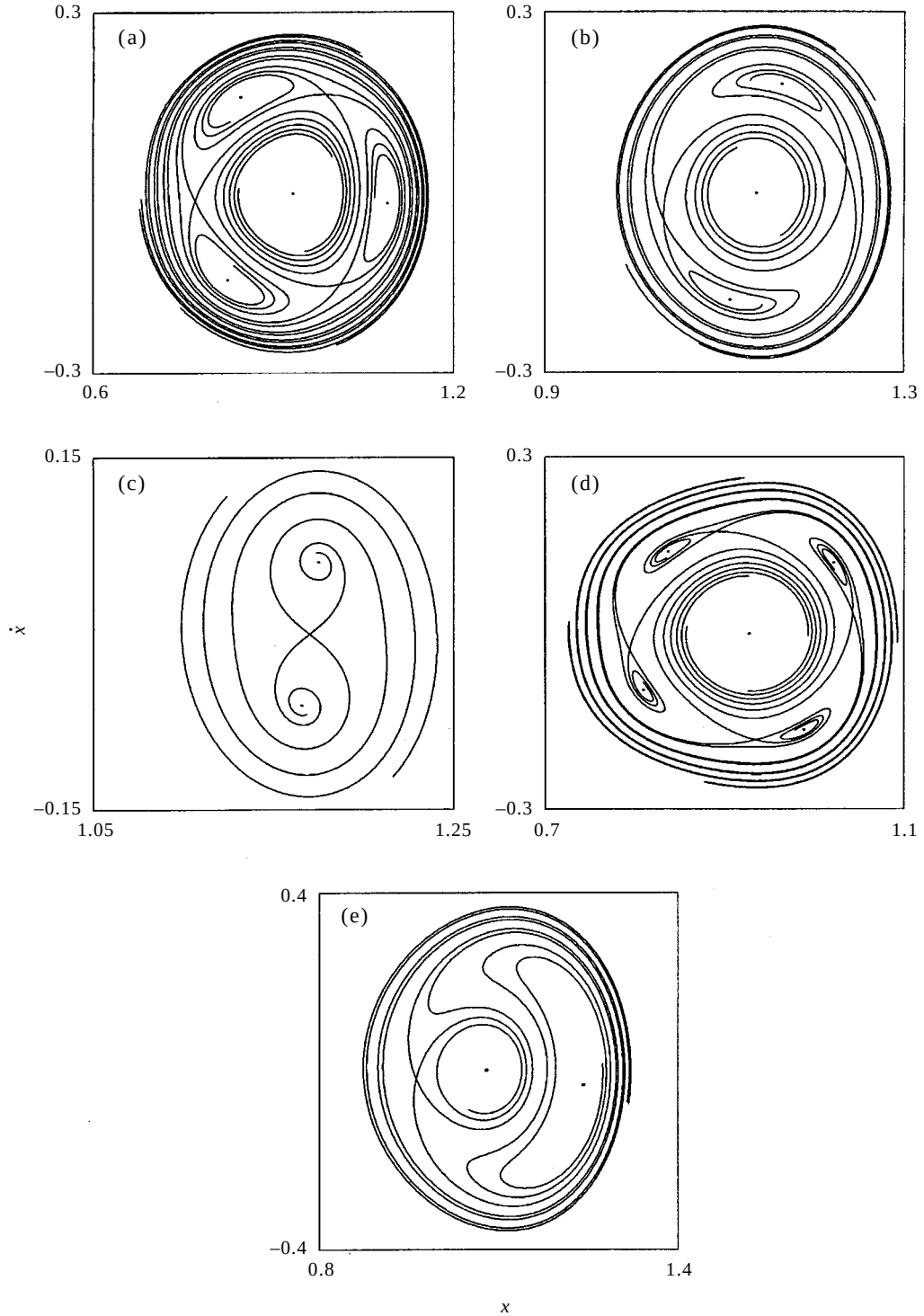

Figure 14. Phase portraits of the Poincaré map P of equation (75) for $\bar{\delta} = 0{\cdot}1$. (a) $\bar{\gamma} = 0{\cdot}15$ and $\omega = 2{\cdot}07$; (b) $\bar{\gamma} = 0{\cdot}15$ and $\omega = 0{\cdot}907$; (c) $\bar{\gamma} = 0{\cdot}185$ and $\omega = 0{\cdot}907$; (d) $\bar{\gamma} = 2$ and $\omega = 5{\cdot}57$; (e) $\bar{\gamma} = 0{\cdot}2$ and $\omega = 0{\cdot}34$. The dots (●) represent stable fixed points or periodic orbits of P. These pictures should be compared with Figures 3(b), 6(b), 6(c), 9(b) and 12(b).

order 3/2 and 2/3 are drawn in Figure 13(a) and (b), respectively, and the bifurcation sets near the fourth-order subharmonic and superharmonic resonances are drawn in Figure 13(c) and (d), respectively. These bifurcation curves were computed for $\varepsilon = 0{\cdot}1$ and $\delta = 1$ (i.e., $\bar{\delta} = 0{\cdot}001$). Condition (74) was used in Figure 13(d). For the purpose of comparison, the corresponding numerical simulation results for equation (75) are also plotted as the broken curves. Here a software called "AUTO" [17] was used to obtain these numerical results. The theoretical predictions are qualitatively in good agreement with the numerical simulation results. It should also be remarked that more accurate theoretical predictions can be obtained if the fourth- or higher-order averaging procedure is used. See reference [8].

Figure 14 shows some numerically computed phase portraits of the Poincaré map P for equation (75), defined as

$$P : (x(0), \dot{x}(0)) \to (x(T), \dot{x}(T)), \tag{76}$$

where $x(t)$ represents a solution of equation (75) and $T = 2\pi/\omega$ is the forcing period. Again, the software "Dynamics" was used here. Thus, the phase portraits of the Poincaré map near the unperturbed centers are very similar to those of the associated averaged systems (see Figures 3(b), 6(b), 6(c), 9(b) and 12(b)) while the periodic orbits of the Poincaré map correspond to fixed points of the averaged systems.

7. CONCLUSIONS

In this paper periodically forced non-linear oscillators of the general form (1) have been studied by applying the third-order averaging method. The ultra-subharmonic resonance motions of order 3/2 and 2/3 near the unperturbed centers were theoretically described. The necessary tedious computations were implemented by using the package of the computer algebra system, Mathematica, recently developed by the author and his co-worker [8]. Several types of bifurcations at which the ultra-subharmonic orbits are created or annihilated were detected. Moreover, the fourth-order subharmonic and superharmonic resonance behavior was discussed. To illustrate the theoretical results, an example was presented for the Duffing oscillator with double well potential. Numerical simulation results were also given and their good agreement with the theoretical predictions was found.

Here special cases of subharmonic, superharmonic and ultra-subharmonic resonances were considered and the third-order averaging method was applied. However, the higher-order averaging method will also reveal other subharmonic, superharmonic and ultra-subharmonic resonance motions, which are found in appropriate numerical simulations as pointed out in section 1, if fourth- or higher-order averaging is carried out. Thus, one may be able to obtain theoretical explanations for complicated dynamical behavior in simple non-linear oscillators.

Our results are valid for a large class of periodically forced oscillators, including weakly non-linear oscillators of the type (2). This implies, along with the results of reference [1], that there exist common bifurcation structures near the ultra-subharmonic resonances as well as the higher-order subharmonic and superharmonic resonances in different systems of the form (1) or (2). In fact, it was shown by numerical computations and experimental measurements that some different systems were proven to have the same bifurcation structures near the primary and subharmonic resonances predicted by the second-order averaging analyses (see references [1, 18]). Hence, numerical or experimental evidence for the above conjecture is expected.

REFERENCES

1. K. YAGASAKI 1996 *Journal of Sound and Vibration* **190**, 587–609. Second-order averaging and Melnikov analyses for forced non-linear oscillators.
2. A. H. NAYFEH and D. T. MOOK 1979 *Nonlinear Oscillations*. New York: Wiley.
3. C. HOLMES and P. HOLMES 1981 *Journal of Sound and Vibration* **78**, 161–174. Second order averaging and bifurcations to subharmonics in Duffing's equation.
4. U. PARLITZ and W. LAUTERBORN 1985 *Physics Letters A* **107**, 351–355. Superstructure in the bifurcation set of the Duffing equation.
5. U. PARLITZ and W. LAUTERBORN 1986 *Zeitschrift für Naturforschung A* **41**, 605–614. Resonances and torsion numbers of driven dissipative nonlinear oscillators.
6. A. NAYFEH 1973 *Perturbation Methods*. New York: Wiley.
7. S.-N. CHOW and J. K. HALE 1982 *Methods of Bifurcation Theory*. New York: Springer-Verlag.
8. K. YAGASAKI and T. ICHIKAWA 1996 (submitted for publication). Higher-order averaging for periodically forced, weakly nonlinear systems.
9. J. MURDOCK 1988 in *Dynamics Reported*, Vol. 1 (J. Kirchgraber and H. O. Walther, editors) 91–172. New York: Wiley. Qualitative theory of nonlinear resonance by averaging and dynamical systems methods.
10. J. MURDOCK 1991 *Perturbations: Theory and Methods*. New York: Wiley.
11. S. WOLFRAM 1991 *Mathematica*, *A System for Doing Mathematics by Computer*. Redwood City, CA: Addison-Wesley; second edition.
12. R. H. RAND and D. ARMBRUSTER 1987 *Perturbation Methods*, *Bifurcation Theory and Computer Algebra*. New York: Springer-Verlag.
13. J. GUCKENHEIMER and P. HOLMES 1983 *Nonlinear Oscillations*, *Dynamical Systems*, *and Bifurcations of Vector Fields*. New York: Springer-Verlag.
14. J. A. SANDERS and F. VERHULST 1985 *Averaging Methods in Nonlinear Dynamical Systems*. New York: Springer-Verlag.
15. S. WIGGINS 1990 *Introduction to Applied Nonlinear Dynamical Systems and Chaos*. New York: Springer-Verlag.
16. E. H. NUSSE and J. A. YORKE 1994 *Dynamics: Numerical Explorations*. New York: Springer-Verlag.
17. E. DOEDEL and J. KERNÉVEZ 1986 *Appl. Math. Reports*, Caltech. AUTO: Software for continuation and bifurcation problems in ordinary differential equations.
18. K. YAGASAKI 1996 *Nonlinear Dynamics* **9**, 391–417. A simple feedback control system: bifurcations of periodic orbits and chaos.

APPENDIX

The functions $\mathbf{w}_{ij}(\theta)$ in equation (24) are given as follows:

$$\mathbf{w}_{10} = \left(-\frac{9a_2\Gamma^2}{8\omega^2}\cos 2\theta + \frac{9a_2\Gamma^2}{32\omega^2}\cos 4\theta - \frac{9a_2\Gamma^2}{64\omega^2}\cos 8\theta, \right.$$

$$\left. \frac{9a_2\Gamma^2}{8\omega^2}\sin 2\theta + \frac{9a_2\Gamma^2}{32\omega^2}\sin 4\theta + \frac{9a_2\Gamma^2}{64\omega^2}\sin 8\theta \right)^{\mathrm{T}}, \tag{A1}$$

$$\mathbf{w}_{11} = \left(\frac{9a_2\Gamma}{4\omega^2}\cos\theta + \frac{9a_2\Gamma}{28\omega^2}\cos 7\theta,\ -\frac{9a_2\Gamma}{4\omega^2}\sin\theta - \frac{3a_2\Gamma}{2\omega^2}\sin 3\theta - \frac{9a_2\Gamma}{28\omega^2}\sin 7\theta \right)^{\mathrm{T}}, \tag{A2}$$

$$\mathbf{w}_{12}(\theta) = \left(-\frac{9a_2\Gamma}{4\omega^2}\sin\theta + \frac{3a_2\Gamma}{2\omega^2}\sin 3\theta - \frac{9a_2\Gamma}{28\omega^2}\sin 7\theta,\ -\frac{9a_2\Gamma}{4\omega^2}\cos\theta - \frac{9a_2\Gamma}{28\omega^2}\cos 7\theta \right)^{\mathrm{T}}, \tag{A3}$$

$$\mathbf{w}_{13}(\theta) = \left(-\frac{9a_2}{16\omega^2}\cos 2\theta - \frac{3a_2}{16\omega^2}\cos 6\theta,\ \frac{27a_2}{16\omega^2}\sin 2\theta + \frac{3a_2}{16\omega^2}\sin 6\theta \right)^{\mathrm{T}}, \tag{A4}$$

$$\mathbf{w}_{14}(\theta) = \left(-\frac{27a_2}{16\omega^2}\cos 2\theta + \frac{3a_2}{16\omega^2}\cos 6\theta,\ \frac{9a_2}{16\omega^2}\sin 2\theta - \frac{3a_2}{16\omega^2}\sin 6\theta \right)^{\mathrm{T}}, \tag{A5}$$

$$\mathbf{w}_{15}(\theta) = \left(-\frac{9a_2}{8\omega^2}\sin 2\theta + \frac{3a_2}{8\omega^2}\sin 6\theta,\ \frac{9a_2}{8\omega^2}\cos 2\theta + \frac{3a_2}{8\omega^2}\cos 6\theta \right)^{\mathrm{T}}, \tag{A6}$$

$$\begin{aligned}\mathbf{w}_{20}(\theta) = \Bigg(& \left[\frac{19737a_2^2\Gamma^3}{1792\omega^4} - \frac{27a_3\Gamma^3}{8\omega^2}\right]\cos\theta - \left[\frac{2565a_2^2\Gamma^3}{1792\omega^4} - \frac{27a_3\Gamma^3}{40\omega^2}\right]\cos 5\theta \\ & + \left[\frac{783a_2^2\Gamma^3}{1792\omega^4} - \frac{9a_3\Gamma^3}{56\omega^2}\right]\cos 7\theta + \left[\frac{1431a_2^2\Gamma^3}{19712\omega^4} + \frac{9a_3\Gamma^3}{88\omega^2}\right]\cos 11\theta, \\ & \left[\frac{19737a_2^2\Gamma^3}{1792\omega^4} - \frac{27a_3\Gamma^3}{8\omega^2}\right]\sin\theta + \left[\frac{2565a_2^2\Gamma^3}{1792\omega^4} - \frac{27a_3\Gamma^3}{40\omega^2}\right]\sin 5\theta \\ & + \left[\frac{783a_2^2\Gamma^3}{1792\omega^4} - \frac{9a_3\Gamma^3}{56\omega^2}\right]\sin 7\theta - \left[\frac{1431a_2^2\Gamma^3}{19712\omega^4} + \frac{9a_3\Gamma^3}{88\omega^2}\right]\sin 11\theta \Bigg)^{\mathrm{T}},\end{aligned} \tag{A7}$$

$$\begin{aligned}\mathbf{w}_{21}(\theta) = \Bigg(& -\left[\frac{3159a_2^2\Gamma^2}{512\omega^4} - \frac{27a_3\Gamma^2}{16\omega^2}\right]\cos 2\theta + \left[\frac{837a_2^2\Gamma^2}{224\omega^4} - \frac{27a_3\Gamma^2}{16\omega^2} + \frac{9\Omega}{8\omega^2}\right]\cos 4\theta \\ & - \left[\frac{1107a_2^2\Gamma^2}{3584\omega^4} + \frac{27a_3\Gamma^2}{80\omega^2}\right]\cos 10\theta, \\ & - \left[\frac{3159a_2^2\Gamma^2}{512\omega^4} - \frac{27a_3\Gamma^2}{16\omega^2}\right]\sin 2\theta - \left[\frac{837a_2^2\Gamma^2}{224\omega^4} - \frac{27a_3\Gamma^2}{16\omega^2} + \frac{9\Omega}{8\omega^2}\right]\sin 4\theta \\ & - \left[\frac{4779a_2^2\Gamma^2}{1792\omega^4} - \frac{9a_3\Gamma^2}{8\omega^2}\right]\sin 6\theta + \left[\frac{1107a_2^2\Gamma^2}{3584\omega^4} + \frac{27a_3\Gamma^2}{80\omega^2}\right]\sin 10\theta \Bigg)^{\mathrm{T}},\end{aligned} \tag{A8}$$

$$\begin{aligned}\mathbf{w}_{22}(\theta) = \Bigg(& -\left[\frac{3159a_2^2\Gamma^2}{512\omega^4} - \frac{27a_3\Gamma^2}{16\omega^2}\right]\sin 2\theta - \left[\frac{837a_2^2\Gamma^2}{224\omega^4} - \frac{27a_3\Gamma^2}{16\omega^2} + \frac{9\Omega}{8\omega^2}\right]\sin 4\theta \\ & + \left[\frac{4779a_2^2\Gamma^2}{1792\omega^4} - \frac{9a_3\Gamma^2}{8\omega^2}\right]\sin 6\theta + \left[\frac{1107a_2^2\Gamma^2}{3584\omega^4} + \frac{27a_3\Gamma^2}{80\omega^2}\right]\sin 10\theta, \\ & \left[\frac{3159a_2^2\Gamma^2}{512\omega^4} - \frac{27a_3\Gamma^2}{16\omega^2}\right]\cos 2\theta - \left[\frac{837a_2^2\Gamma^2}{224\omega^4} - \frac{27a_3\Gamma^2}{16\omega^2} + \frac{9\Omega}{8\omega^2}\right]\cos 4\theta\end{aligned}$$

$$+\left[\frac{1107a_2^2\,\Gamma^2}{3584\omega^4}+\frac{27a_3\,\Gamma^2}{80\omega^2}\right]\cos 10\theta\Bigg)^{\mathrm{T}}, \tag{A9}$$

$$\mathbf{w}_{23}(\theta)=\Bigg(\left[\frac{2349a_2^2\,\Gamma}{224\omega^4}-\frac{27a_3\,\Gamma}{8\omega^2}\right]\cos\theta-\left[\frac{81a_2^2\,\Gamma}{32\omega^4}-\frac{9a_3\,\Gamma}{8\omega^2}\right]\cos 3\theta$$

$$-\left[\frac{297a_2^2\,\Gamma}{224\omega^4}-\frac{27a_3\,\Gamma}{40\omega^2}\right]\cos 5\theta+\left[\frac{99a_2^2\,\Gamma}{224\omega^4}+\frac{3a_3\,\Gamma}{8\omega^2}\right]\cos 9\theta,$$

$$\left[\frac{7047a_2^2\,\Gamma}{224\omega^4}-\frac{81a_3\,\Gamma}{8\omega^2}\right]\sin\theta+\left[\frac{81a_2^2\,\Gamma}{32\omega^4}-\frac{9a_3\,\Gamma}{8\omega^2}\right]\sin 3\theta$$

$$+\left[\frac{891a_2^2\,\Gamma}{224\omega^4}-\frac{81a_3\,\Gamma}{40\omega^2}\right]\sin 5\theta-\left[\frac{99a_2^2\,\Gamma}{224\omega^4}+\frac{3a_3\,\Gamma}{8\omega^2}\right]\sin 9\theta\Bigg)^{\mathrm{T}}, \tag{A10}$$

$$\mathbf{w}_{24}(\theta)=\Bigg(\left[\frac{7047a_2^2\,\Gamma}{224\omega^4}-\frac{81a_3\,\Gamma}{8\omega^2}\right]\cos\theta+\left[\frac{81a_2^2\,\Gamma}{32\omega^4}-\frac{9a_3\,\Gamma}{8\omega^2}\right]\cos 3\theta$$

$$-\left[\frac{891a_2^2\,\Gamma}{224\omega^4}-\frac{81a_3\,\Gamma}{40\omega^2}\right]\cos 5\theta-\left[\frac{99a_2^2\,\Gamma}{224\omega^4}+\frac{3a_3\,\Gamma}{8\omega^2}\right]\cos 9\theta,$$

$$\left[\frac{2349a_2^2\,\Gamma}{224\omega^4}-\frac{27a_3\,\Gamma}{8\omega^2}\right]\sin\theta-\left[\frac{81a_2^2\,\Gamma}{32\omega^4}-\frac{9a_3\,\Gamma}{8\omega^2}\right]\sin 3\theta$$

$$+\left[\frac{297a_2^2\,\Gamma}{224\omega^4}-\frac{27a_3\,\Gamma}{40\omega^2}\right]\sin 5\theta+\left[\frac{99a_2^2\,\Gamma}{224\omega^4}+\frac{3a_3\,\Gamma}{8\omega^2}\right]\sin 9\theta\Bigg)^{\mathrm{T}}, \tag{A11}$$

$$\mathbf{w}_{25}(\theta)=\Bigg(\left[\frac{-2349a_2^2\,\Gamma}{112\omega^4}+\frac{27a_3\,\Gamma}{4\omega^2}\right]\sin\theta+\left[\frac{81a_2^2\,\Gamma}{16\omega^4}-\frac{9a_3\,\Gamma}{4\omega^2}\right]\sin 3\theta$$

$$-\left[\frac{297a_2^2\,\Gamma}{112\omega^2}-\frac{27a_3\,\Gamma}{20\omega^2}\right]\sin 5\theta-\left[\frac{99a_2^2\,\Gamma}{112\omega^4}+\frac{3a_3\,\Gamma}{4\omega^2}\right]\sin 9\theta,$$

$$-\left[\frac{2349a_2^2\,\Gamma}{112\omega^4}-\frac{27a_3\,\Gamma}{4\omega^2}\right]\cos\theta+\left[\frac{81a_2^2\,\Gamma}{16\omega^4}-\frac{9a_3\,\Gamma}{4\omega^2}\right]\cos 3\theta$$

$$+\left[\frac{297a_2^2\,\Gamma}{112\omega^4}-\frac{27a_3\,\Gamma}{20\omega^2}\right]\cos 5\theta-\left[\frac{99a_2^2\,\Gamma}{112\omega^4}+\frac{3a_3\,\Gamma}{4\omega^2}\right]\cos 9\theta\Bigg)^{\mathrm{T}}, \tag{A12}$$

$$\mathbf{w}_{26}(\theta)=\Bigg(\left[\frac{27a_2^2}{32\omega^4}-\frac{9a_3}{16\omega^2}\right]\cos 4\theta-\left[\frac{27a_2^2}{128\omega^4}+\frac{9a_3}{64\omega^2}\right]\cos 8\theta,$$

$$-\left[\frac{27a_2^2}{16\omega^4}-\frac{9a_3}{8\omega^2}\right]\sin 4\theta+\left[\frac{27a_2^2}{128\omega^4}+\frac{9a_3}{64\omega^2}\right]\sin 8\theta\Bigg)^{\mathrm{T}}, \tag{A13}$$

$$\mathbf{w}_{27}(\theta)=\Bigg(-\left[\frac{27a_2^2}{16\omega^4}-\frac{9a_3}{8\omega^2}\right]\sin 4\theta-\left[\frac{27a_2^2}{128\omega^4}+\frac{9a_3}{64\omega^2}\right]\sin 8\theta,$$

$$-\left[\frac{27a_2^2}{32\omega^4}-\frac{9a_3}{16\omega^2}\right]\cos 4\theta-\left[\frac{27a_2^2}{128\omega^4}+\frac{9a_3}{64\omega^2}\right]\cos 8\theta\Bigg)^{\mathrm{T}}, \tag{A14}$$

$$\mathbf{w}_{28}(\theta)=\Bigg(\left[\frac{81a_2^2}{128\omega^4}+\frac{27a_3}{64\omega^2}\right]\sin 8\theta,\ -\left[\frac{81a_2^2}{32\omega^4}-\frac{27a_3}{16\omega^2}\right]\cos 4\theta$$

$$+\left[\frac{81a_2^2}{128\omega^4}+\frac{27a_3}{64\omega^2}\right]\cos 8\theta\Bigg)^{\mathrm{T}}, \tag{A15}$$

$$\mathbf{w}_{29}(\theta)=\Bigg(\left[\frac{81a_2^2}{32\omega^4}-\frac{27a_3}{16\omega^2}\right]\cos 4\theta+\left[\frac{81a_2^2}{128\omega^4}+\frac{27a_3}{64\omega^2}\right]\cos 8\theta,$$

$$-\left[\frac{81a_2^2}{128\omega^4}+\frac{27a_3}{64\omega^2}\right]\sin 8\theta\Bigg)^{\mathrm{T}}, \tag{A16}$$

where the superscript $^{\mathrm{T}}$ represents the transpose operator.